Supplementary Information for

Tris(8-methoxy-2-quinolylmethyl)amine (8-MeOTQA) as a highly fluorescent Zn^{2+} probe prepared by convenient C_3-symmetric tripodal amine synthesis

Yuji Mikata,[a,b,*] Yuki Nodomi,[b] Risa Ohnishi,[b] Asako Kizu[b] and Hideo Konno[c]

[a]KYOUSEI Science Center and [b]Department of Chemistry, Faculty of Science, Nara Women's University, Nara 630-8506, Japan and [c]National Institute of Advanced Industrial Science and Technology (AIST), 1-1-1 Higashi, Tsukuba, Ibaraki 305-8565, Japan

Table S1 Crystallographic Data for Tris(2,4,6-trimethylbenzyl)amine (**2**) and 8-MeOTQA·0.5CH_2Cl_2 (**4**·0.5CH_2Cl_2)

	2	8-MeOTQA·0.5CH_2Cl_2 (**4**·0.5CH_2Cl_2)
Formula	$C_{30}H_{39}N$	$C_{33.5}H_{31}ClN_4O_3$
FW	413.64	573.09
Crystal system	monoclinic	triclinic
Space group	$P2_1/c$	P-1
a, Å	10.2132(4)	13.6378(18)
b, Å	30.9988(11)	14.5501(17)
c, Å	16.2427(6)	15.854(2)
α, deg	90	76.043(6)
β, deg	95.006(3)	82.248(6)
γ, deg	90	69.739(6)
V, Å^3	5122.8(4)	2859.5(7)
Z	8	4
D_{calc}, g cm^{-3}	1.073	1.331
μ, mm^{-1}	0.0607	0.1758
$2\theta_{max}$, deg	55.0	55.0
temp, K	153	153
no. reflns collected	50925	23430
no. reflns used	11658	12543
no. of params	793	748
R_{int}	0.0450	0.0294
Final $R1$ ($I > 2\sigma(I)$)[a]	0.0685	0.0757
$wR2$ (all data)[b]	0.1693	0.2382
GOF	1.096	1.065

[a] $R1 = \Sigma||F_o| - |F_c||/\Sigma|F_o|$. [b] $wR2 = [\Sigma w[(F_o^2 - F_c^2)^2]/\Sigma[w(F_o^2)^2]]^{1/2}$.

Table S2 Crystallographic Data for [Zn(8-MeOTQA)]$(ClO_4)_2$ and [Cd(8-MeOTQA)]$(ClO_4)_2$

	[Zn(8-MeOTQA)]$(ClO_4)_2$	[Cd(8-MeOTQA)]$(ClO_4)_2$
Formula	$C_{33}H_{30}Cl_2N_4O_{11}Zn$	$C_{33}H_{30}CdCl_2N_4O_{11}$
FW	794.91	841.94
Crystal system	monoclinic	monoclinic
Space group	$P2_1/c$	$P2_1/c$
a, Å	18.484(2)	18.248(5)
b, Å	11.4954(13)	11.367(3)
c, Å	15.595(2)	15.943(5)
β, deg	105.6890(16)	95.105(3)
V, Å^3	3190.3(7)	3293.7(15)
Z	4	4
D_{calc}, g cm^{-3}	1.655	1.698
μ, mm^{-1}	1.0092	0.8957
$2\theta_{max}$, deg	55.0	55.0
temp, K	153	153
no. reflns collected	23966	32773
no. reflns used	7162	7560
no. of params	580	460
R_{int}	0.0210	0.0409
Final $R1$ ($I > 2\sigma(I)$)[a]	0.0334	0.0453
$wR2$ (all data)[b]	0.0891	0.1185
GOF	1.061	1.078

[a] $R1 = \Sigma||F_o| - |F_c||/\Sigma|F_o|$. [b] $wR2 = [\Sigma w[(F_o^2 - F_c^2)^2]/\Sigma[w(F_o^2)^2]]^{1/2}$.

Table S3 Crystallographic Data for [Zn(6-MeOTQA)(DMF)(ClO_4)]ClO_4·0.5H_2O and [Zn(8-MeOBQPA)(CH_3OH)](ClO_4)$_2$·0.5H_2O

	[Zn(6-MeOTQA)(DMF)-(ClO_4)]ClO_4·0.5H_2O	[Zn(8-MeOBQPA)-(CH_3OH)](ClO_4)$_2$·0.5H_2O
Formula	$C_{36}H_{38}Cl_2N_5O_{12.5}Zn$	$C_{29}H_{31}Cl_2N_4O_{11.5}Zn$
FW	877.01	755.87
Crystal system	monoclinic	triclinic
Space group	*Cc*	*P*-1
a, Å	19.446(5)	12.5269(17)
b, Å	14.257(3)	14.684(2)
c, Å	15.252(4)	20.826(3)
α, deg	90	72.888(7)
β, deg	116.370(2)	69.124(7)
γ, deg	90	64.913(6)
V, Å^3	3788.2(17)	3195.0(8)
Z	4	4
D_{calc}, g cm^{-3}	1.538	1.571
μ, mm^{-1}	0.8613	1.0041
$2\theta_{max}$, deg	55.0	55.0
temp, K	153	153
no. reflns collected	14423	25181
no. reflns used	6352	13957
no. of params	532	904
R_{int}	0.0236	0.0257
Final *R*1 ($I > 2\sigma(I)$)[a]	0.0396	0.0501
*wR*2 (all data)[b]	0.1017	0.1321
GOF	1.082	1.081

[a] $R1 = \Sigma||F_o| - |F_c||/\Sigma|F_o|$. [b] $wR2 = [\Sigma w[(F_o^2 - F_c^2)^2]/\Sigma[w(F_o^2)^2]]^{1/2}$.

Table S4 Crystallographic Data for [Cd(8-MeOBQPA)(CH_3OH)](ClO_4)$_2$·CH_3OH

	[Cd(8-MeOBQPA)(CH_3OH)](ClO_4)$_2$·CH_3OH
Formula	$C_{30}H_{34}CdCl_2N_4O_{12}$
FW	825.93
Crystal system	monoclinic
Space group	$P2_1/c$
a, Å	17.838(3)
b, Å	11.9318(16)
c, Å	15.668(2)
β, deg	97.0190(17)
V, Å^3	3309.8(8)
Z	4
D_{calc}, g cm^{-3}	1.657
μ, mm^{-1}	0.8914
$2\theta_{max}$, deg	55.0
temp, K	153
no. reflns collected	25209
no. reflns used	7549
no. of params	446
R_{int}	0.0207
Final $R1$ ($I > 2\sigma(I)$)[a]	0.0440
$wR2$ (all data)[b]	0.1201
GOF	1.066

[a] $R1 = \Sigma||F_o| - |F_c||/\Sigma|F_o|$. [b] $wR2 = [\Sigma w[(F_o^2 - F_c^2)^2]/\Sigma[w(F_o^2)^2]]^{1/2}$.

Table S5 Comparison of Fluorescence Sensing Properties of 8-Hydroxy- or 8-Alkoxy-2-aminomethylquinoline Derivatives

Compound[a]	I_{Zn}/I_0	I_{Cd}/I_{Zn}(%)	ϕ_{Zn}	Solvent	Reference
8-MeOTQA(**4**)	16	16	0.51	DMF-H_2O (1:1)	-
A	-	75	-	MeOH (0.01 M NaOAc)	b
B	-	15	-	MeOH (0.01 M NaOAc)	b
C	-	~50	-	MeOH (0.01 M NaOAc)	c
D	7	44	-	CH_3CN-HEPES (4:1)	d
E	17	~250	-	10 mM HEPES buffer	e
F	0.5	~120	-	10 mM HEPES buffer	e
	13	-	0.03	50 mM HEPES-DMSO (99:1)	h
G	~10	~130	0.24	50 mM HEPES buffer	f
	11	-	0.24	50 mM HEPES-DMSO (99:1)	j
H	~6	~100	0.43	25 mM HEPES buffer	g
I	~4	~200	0.24	25 mM HEPES-DMSO (95:5)	h
J	~5	~120	0.49	25 mM HEPES-DMSO (95:5)	h
K	~6	~200	0.65	25 mM HEPES-DMSO (95:5)	h
L	~9	~13	-	MeOH-H_2O (1:1)	i
M	3.6	-	0.03	50 mM HEPES-DMSO (99:1)	j

[a] See Chart S1.
[b] *J. Org. Chem.*, 2001, **66**, 4752.
[c] *Anal. Sci.*, 2003, **19**, 1353.
[d] *Dalton Trans.*, 2004, 2771.
[e] *Chem. Eur. J.*, 2006, **12**, 9066.
[f] *J. Am. Chem. Soc.*, 2006, **128**, 3854.
[g] *Org. Lett.*, 2007, **9**, 4995.
[h] *Inorg. Chem.*, 2008, **47**, 4310.
[i] *Dalton Trans.*, 2013, **42**, 14516.
[j] *Polyhedron*, 2013, **58**, 85.

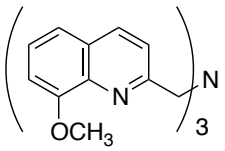

8-MeOTQA (**4**)

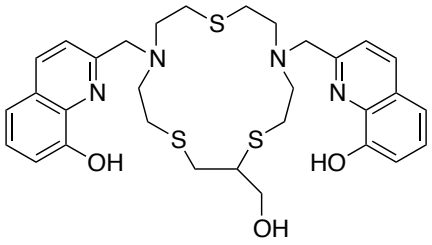

A

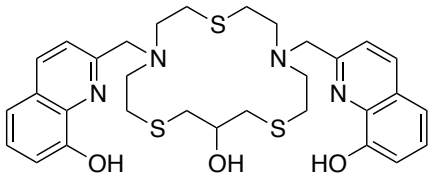

B

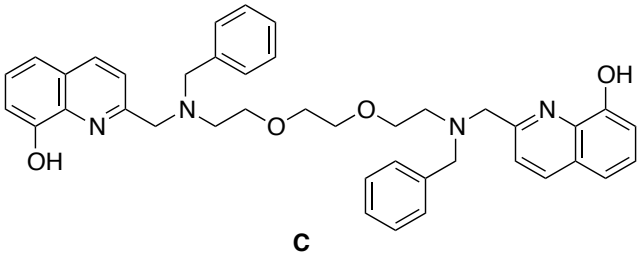

C

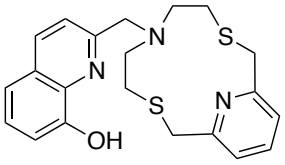

D

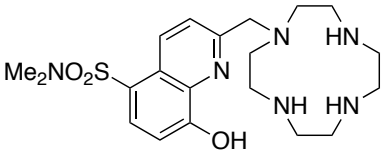

E

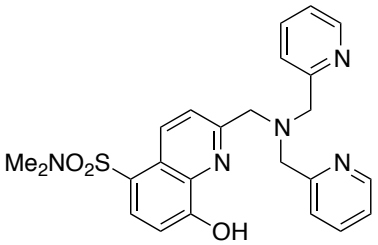

F

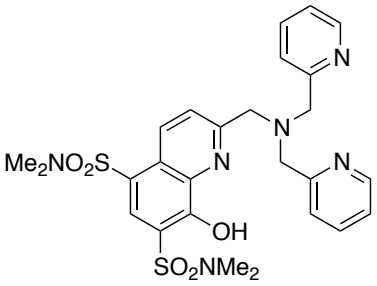

G

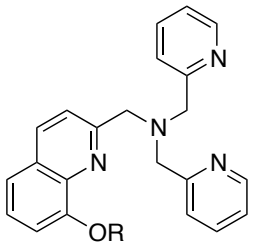

R = CH_2CO_2Na : **H**
H : **I**
2-pycolyl : **J**
$CH_2CH_2CH_2CO_2Na$: **K**

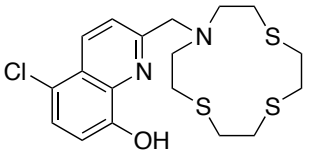

L

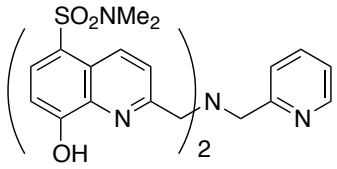

M

Chart S1

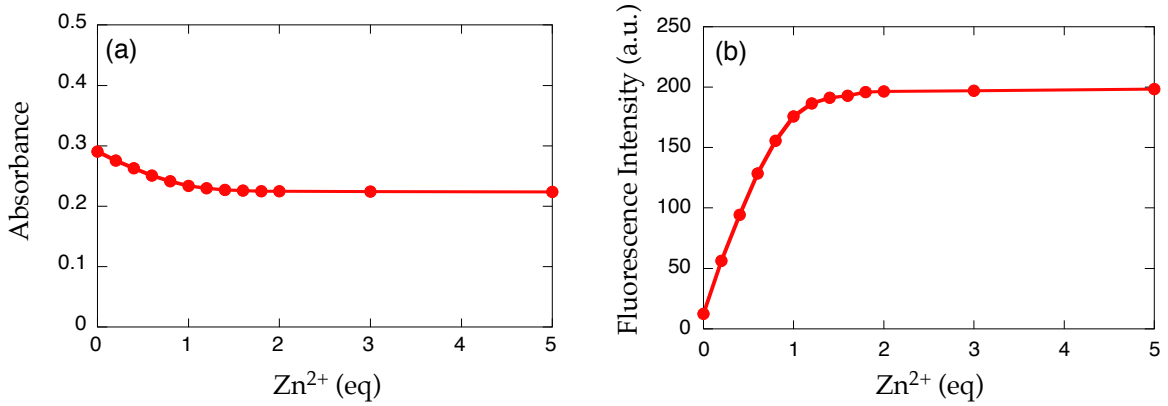

Fig. S1 (a) Absorbance (at 304 nm) and (b) fluorescence (at 442 nm) spectral changes for 34 μM 8-MeOTQA (**4**) in the presence of increasing amount of Zn^{2+} in DMF-H_2O (1:1) (λ_{ex} = 335 nm, 25 °C).

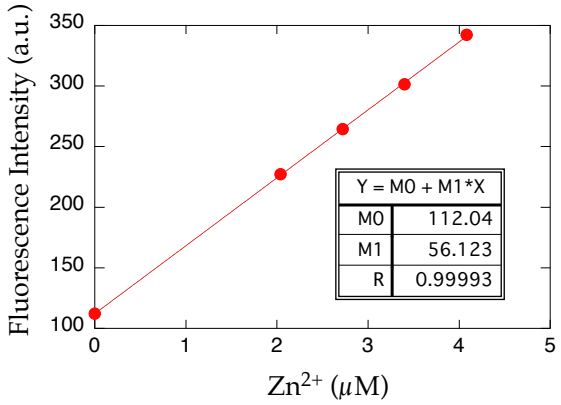

Fig. S2 Estimation of LOD (limit of detection) for Zn^{2+} with 8-MeOTQA in DMF-H_2O (1:1). The 3σ value (σ corresponds to standard deviation from 5 measurements) of blank solution (34 μM 8-MeOTQA) is 0.191 in fluorescence intensity unit, which corresponds to 3.4 nM from the slope of the liner dynamic fluorescence intensity plot (*k*) shown above (LOD = 3σ/*k*).

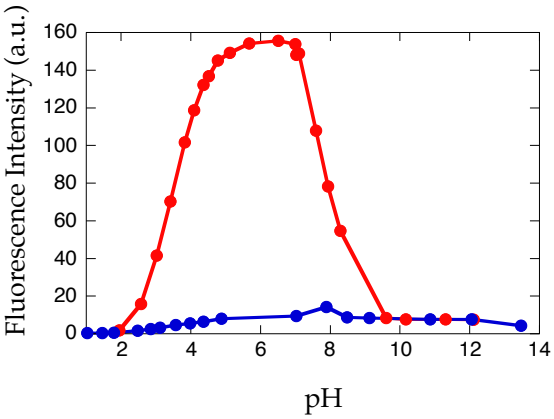

Fig. S3 Effect of pH on fluorescence intensity of 34 μM 8-MeOTQA (**4**) at 442 nm in the absence (blue) and presence (red) of 1 equiv. of Zn^{2+} in DMF-H_2O (1:1) at 25 °C (λ_{ex} = 335 nm).

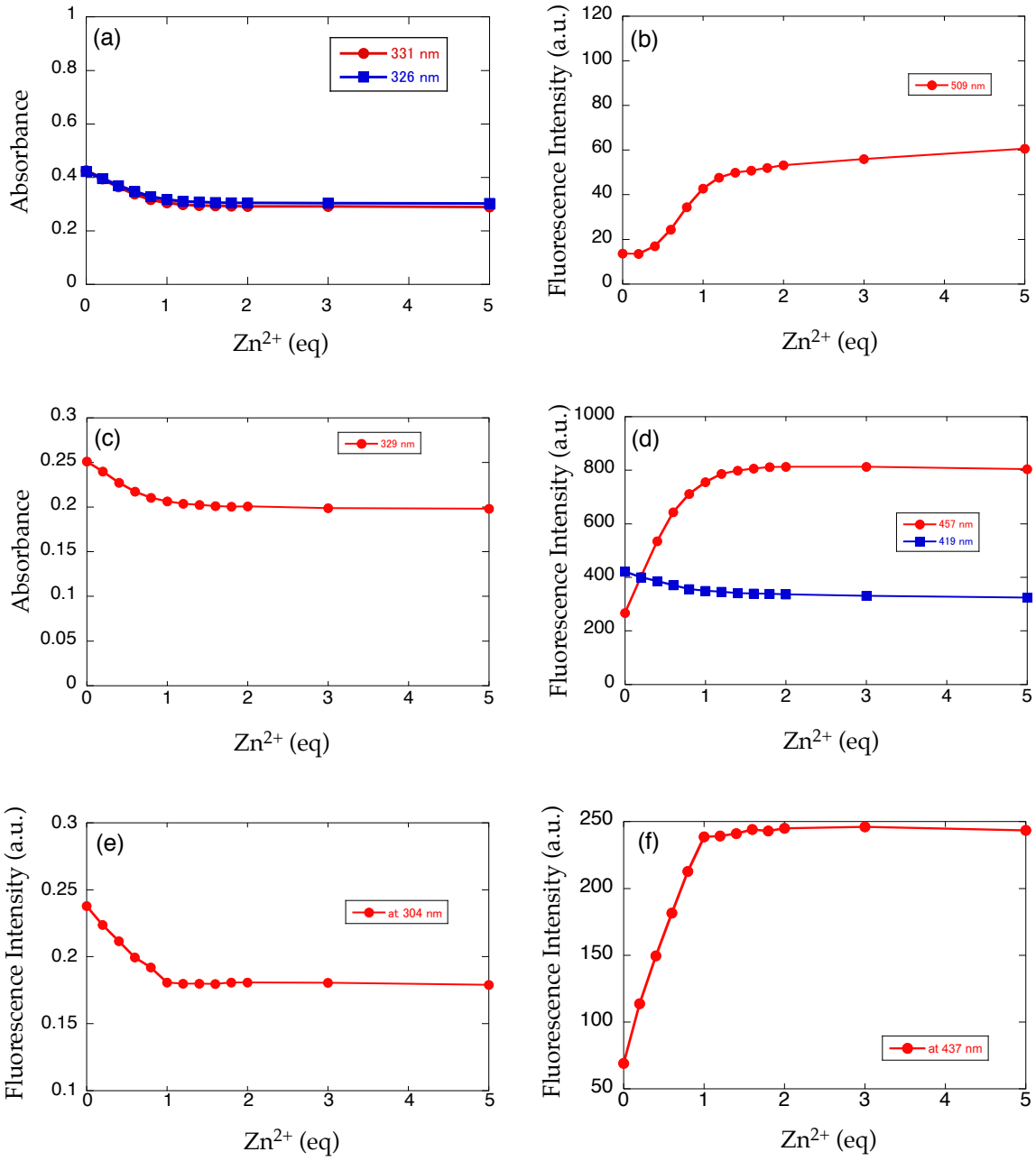

Fig. S4 (a, c, e) Absorbance and (b, d, f) fluorescence spectral changes for 34 μM (a, b) 6-MeOTQA (**3**), (c, d) 6,8-DiMeOTQA (**5**) and (e, f) 8-MeOBQPA (**8**) in the presence of increasing amount of Zn^{2+} in DMF-H_2O (1:1) at 25 °C (λ_{ex} = 332 nm for 6-MeOTQA; 347 nm for 6,8-DiMeOTQA; 335 nm for 8-MeOBQPA).

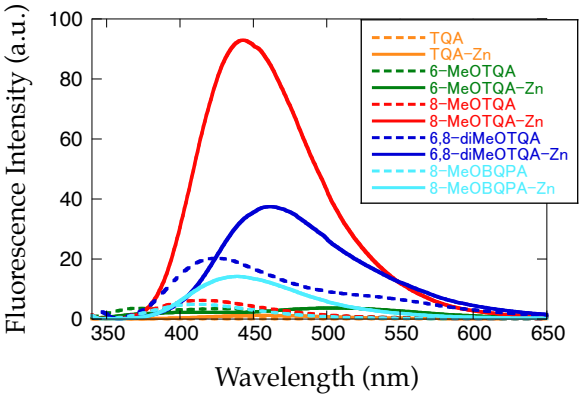

Fig. S5 Comparison of fluorescence spectra of 34 μM TQA (orange), 6-MeOTQA (**3**) (green), and 8-MeOTQA (**4**) (red), 6,8-DiMeOTQA (**5**) (blue) and 8-MeOBQPA (**8**) (light blue) in the presence (solid lines) and absence (broken lines) of 1 equiv. of Zn^{2+} in DMF-H_2O (1:1) at 25 °C (λ_{ex} = 317 nm for TQA; 332 nm for 6-MeOTQA; 335 nm for 8-MeOTQA and 8-MeOBQPA; 347 nm for 6,8-DiMeOTQA).

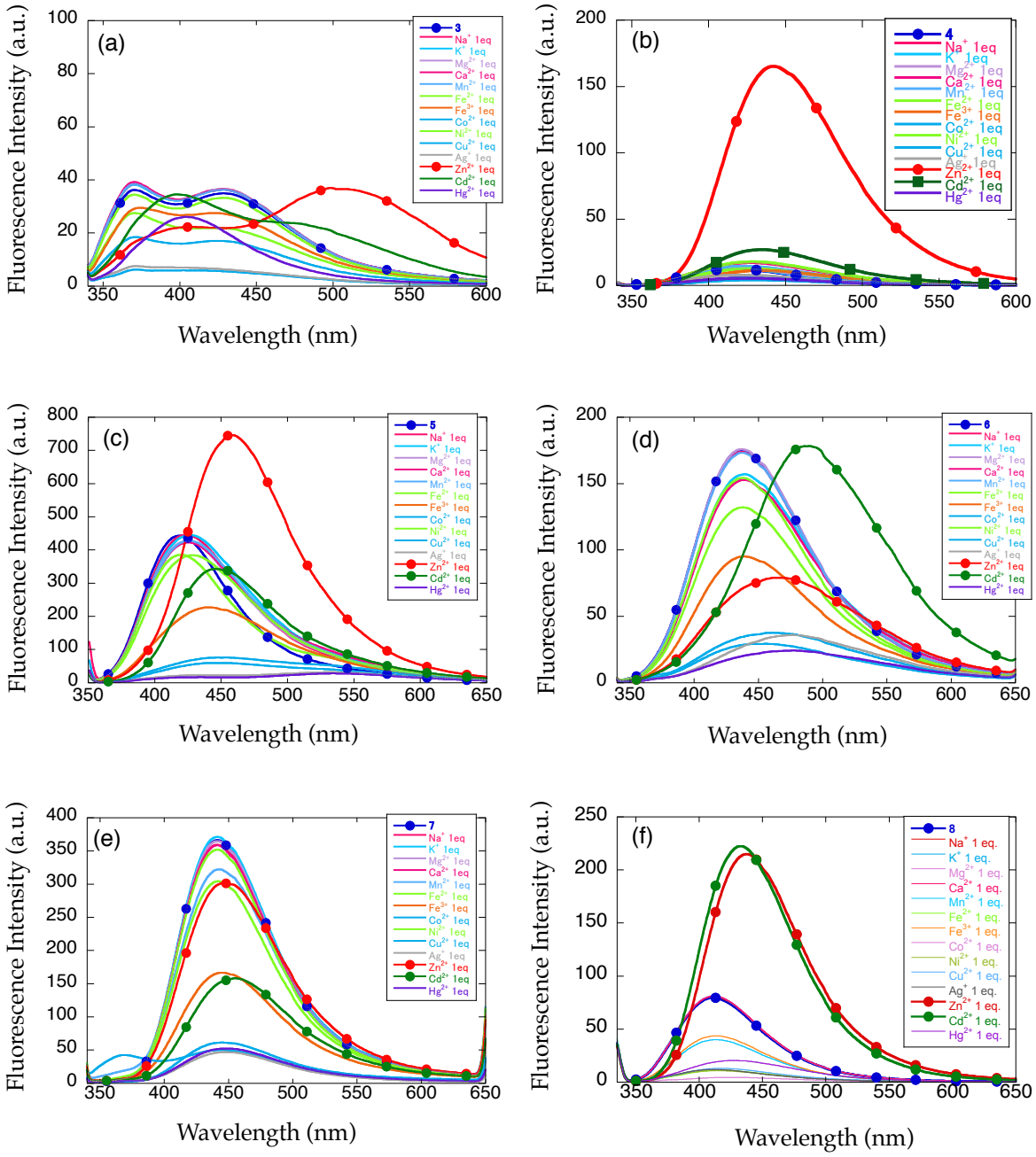

Fig. S6 Comparison of fluorescence spectra of 34 μM (a) 6-MeOTQA (**3**), (b) 8-MeOTQA (**4**), (c) 6,8-DeiMeOTQA (**5**), (d) 5,6,7-TriMeOTQA (**6**), (e) 8-MeSTQA (**7**) and (f) 8-MeOBQPA (**8**) in the presence of 1 equiv. of various metal ions in DMF-H_2O (1:1) at 25 °C.

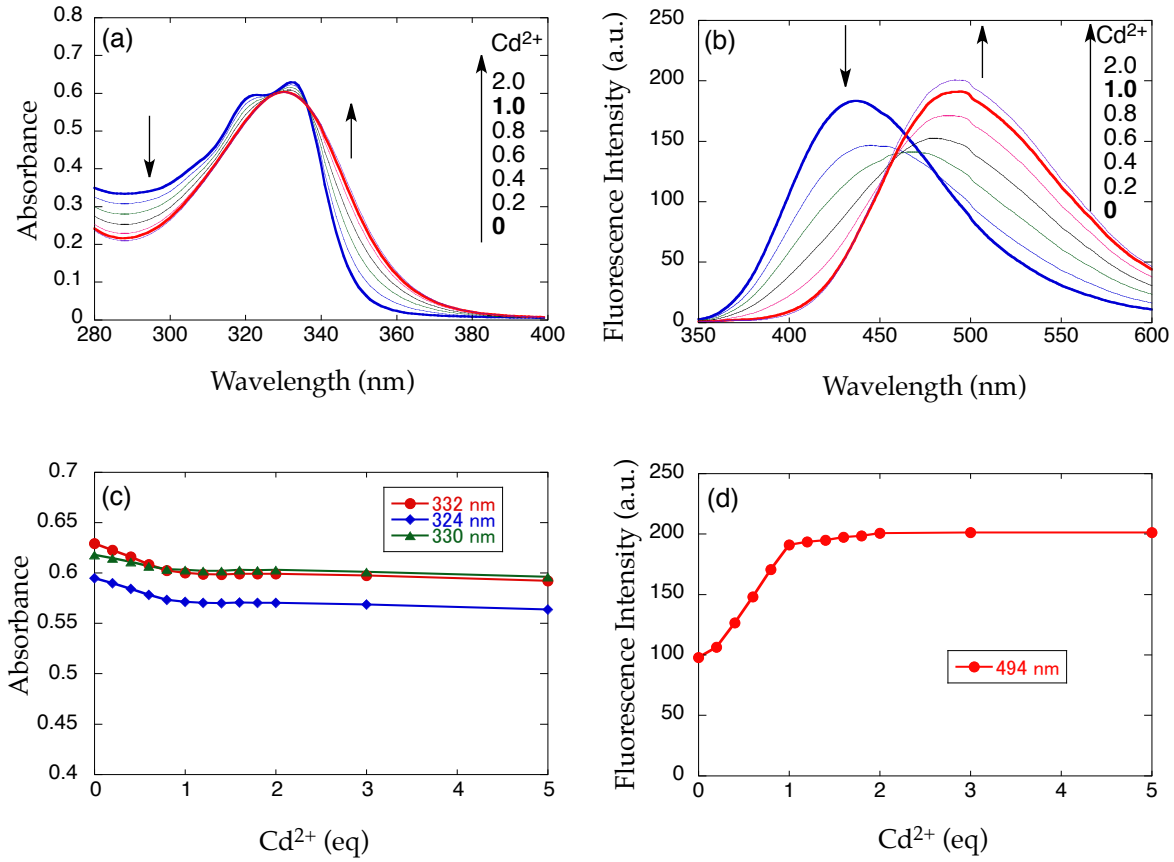

Fig. S7 Absorption and fluorescence spectral changes of 34 μM 5,6,7-TriMeOTQA (**6**) in DMF-H_2O (1:1) in the presence of Cd^{2+} (λ_{ex} = 332 nm, 25 °C). (a, c) Absorbance changes upon addition of Cd^{2+}. (b, d) Fluorescence changes upon addition of Cd^{2+}.

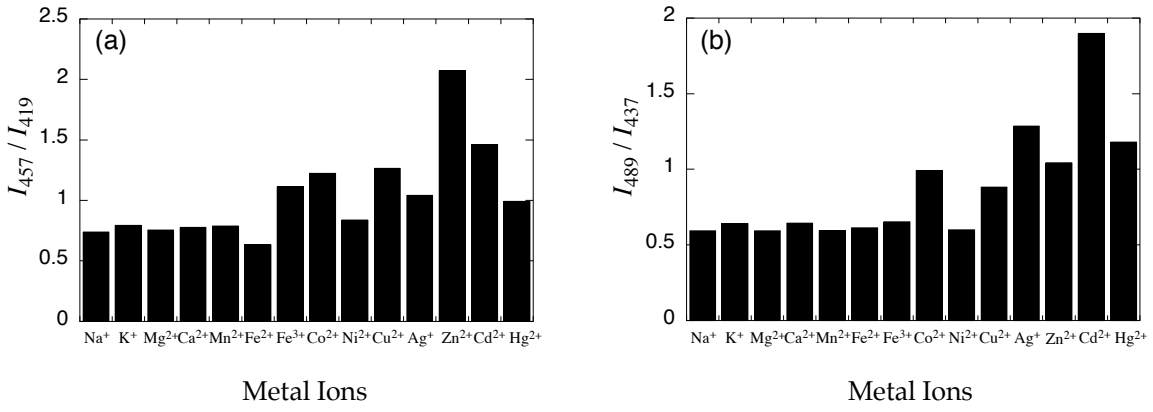

Fig. S8 The relative fluorescence intensity of (a) 6,8-DiMeOTQA (**5**) and (b) 5,6,7-TriMeOTQA (**6**) in the presence of 1 equiv. of metal ions in DMF-H_2O (1:1) at 25 °C.

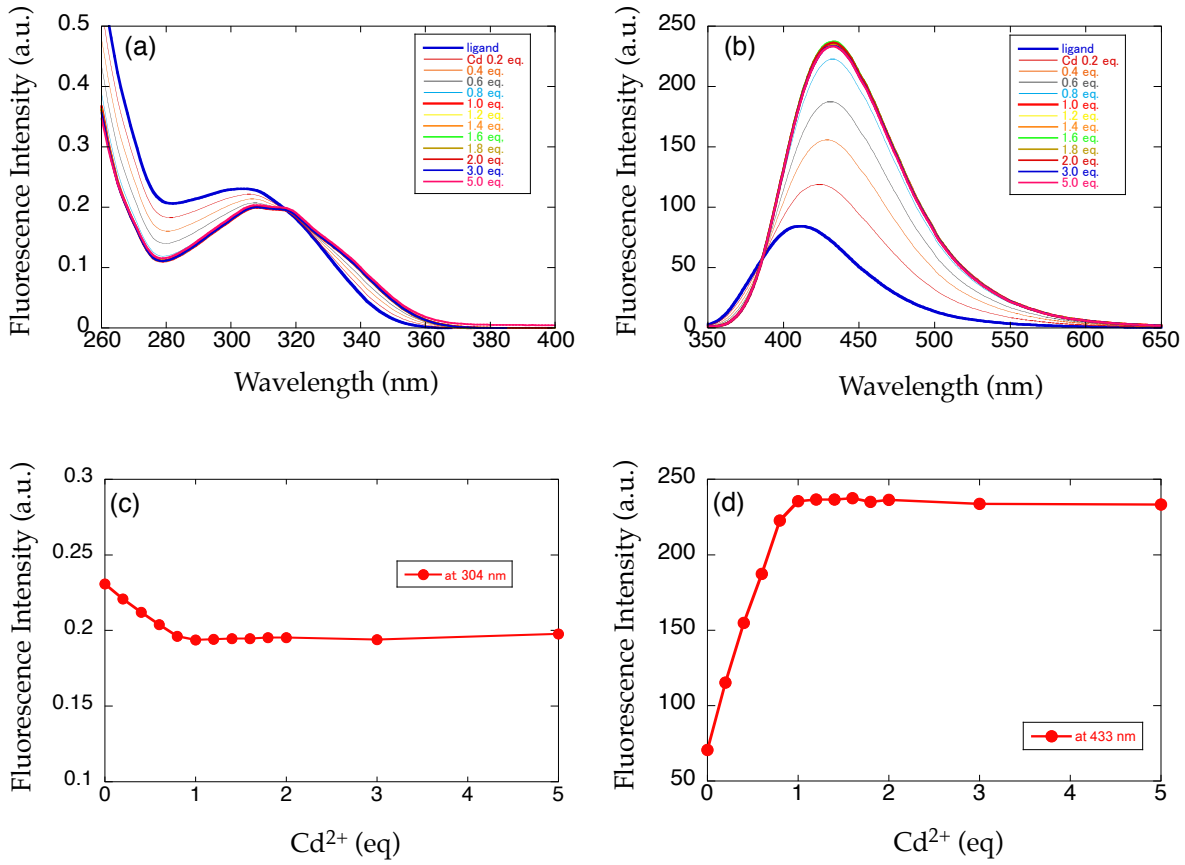

Fig. S9 Absorption and fluorescence spectral changes of 34 μM 8-MeOBQPA (**8**) in the presence of Cd^{2+} in DMF-H_2O (1:1) (λ_{ex} = 335 nm, 25 °C). (a, c) Absorbance changes upon addition of Cd^{2+}. (b, d) Fluorescence changes upon addition of Cd^{2+}.

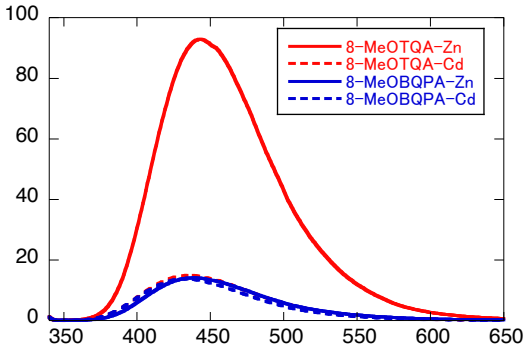

Fig. S10 Comparison of fluorescence spectra for 34 μM 8-MeOTQA (**4**) (red) and 8-MeOBQPA (**8**) (blue) in DMF-H_2O (1:1) in the presence of 1 equiv. of Zn^{2+} (solid lines) or Cd^{2+} (broken lines) (λ_{ex} = 335 nm, 25 °C).

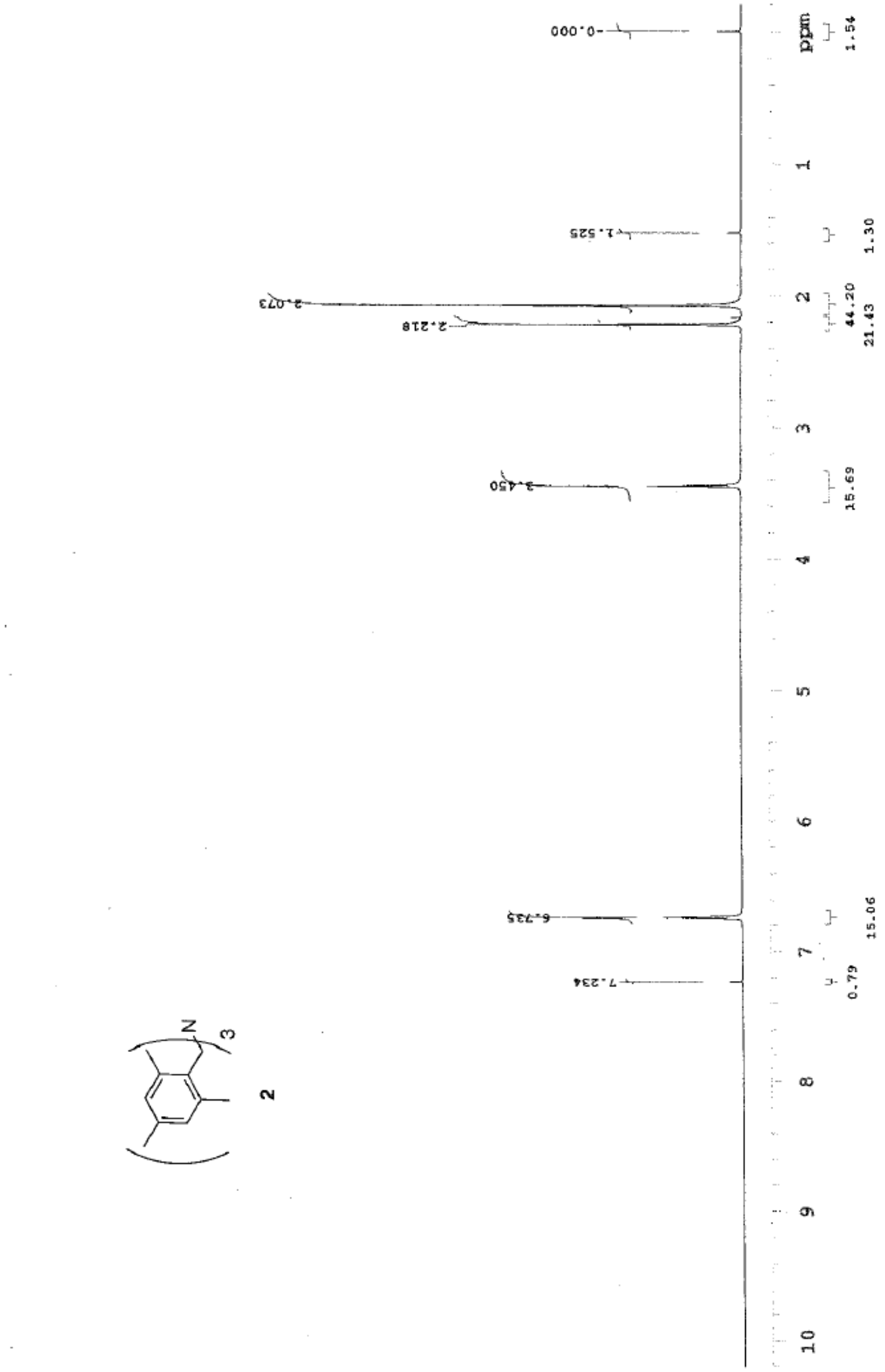

Fig. S11 ^{1}H NMR spectrum of **2** in $CDCl_3$.

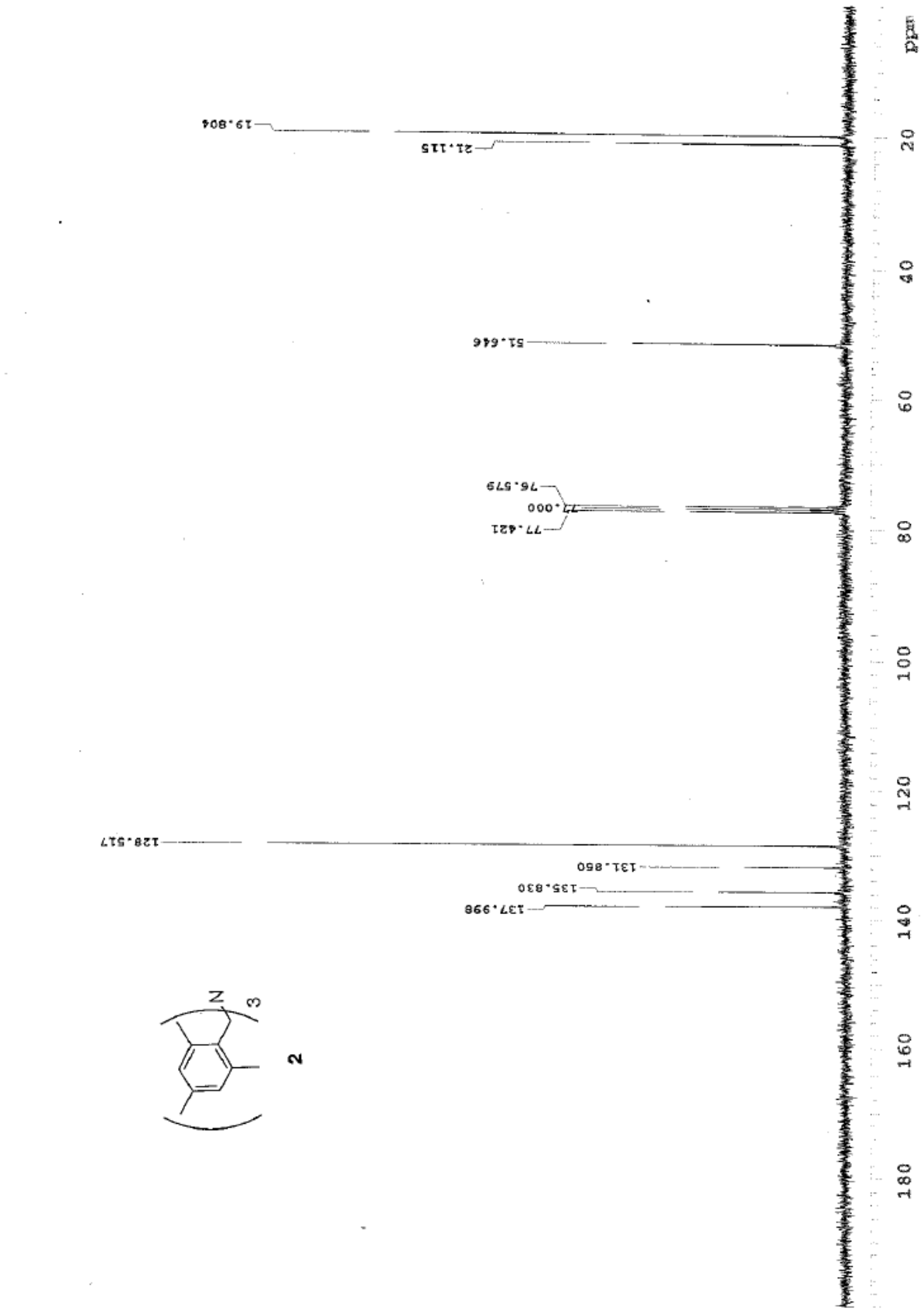

Fig. S12 ^{13}C NMR spectrum of **2** in $CDCl_3$.

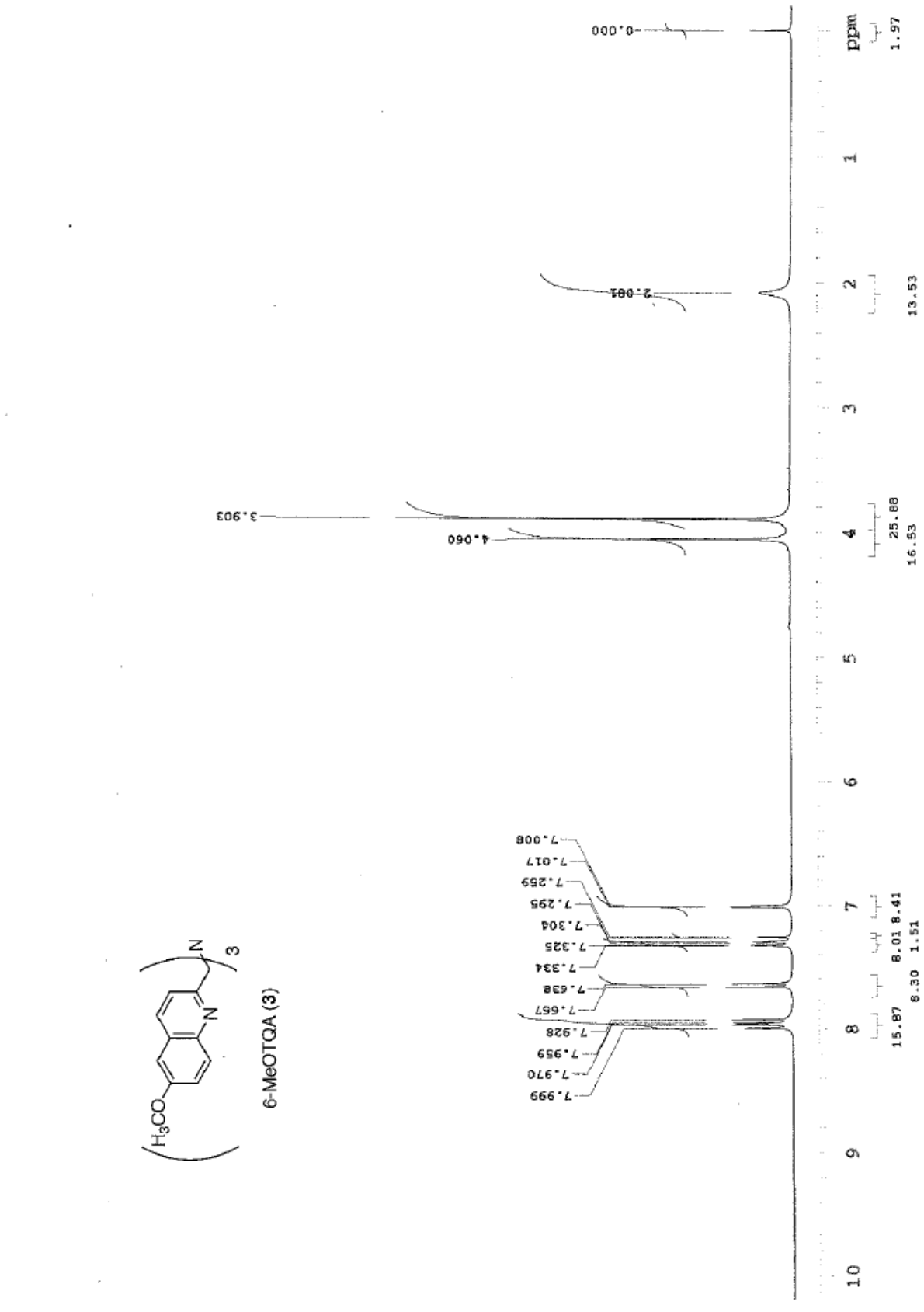

Fig. S13 ^{1}H NMR spectrum of 6-MeOTQA (**3**) in $CDCl_3$.

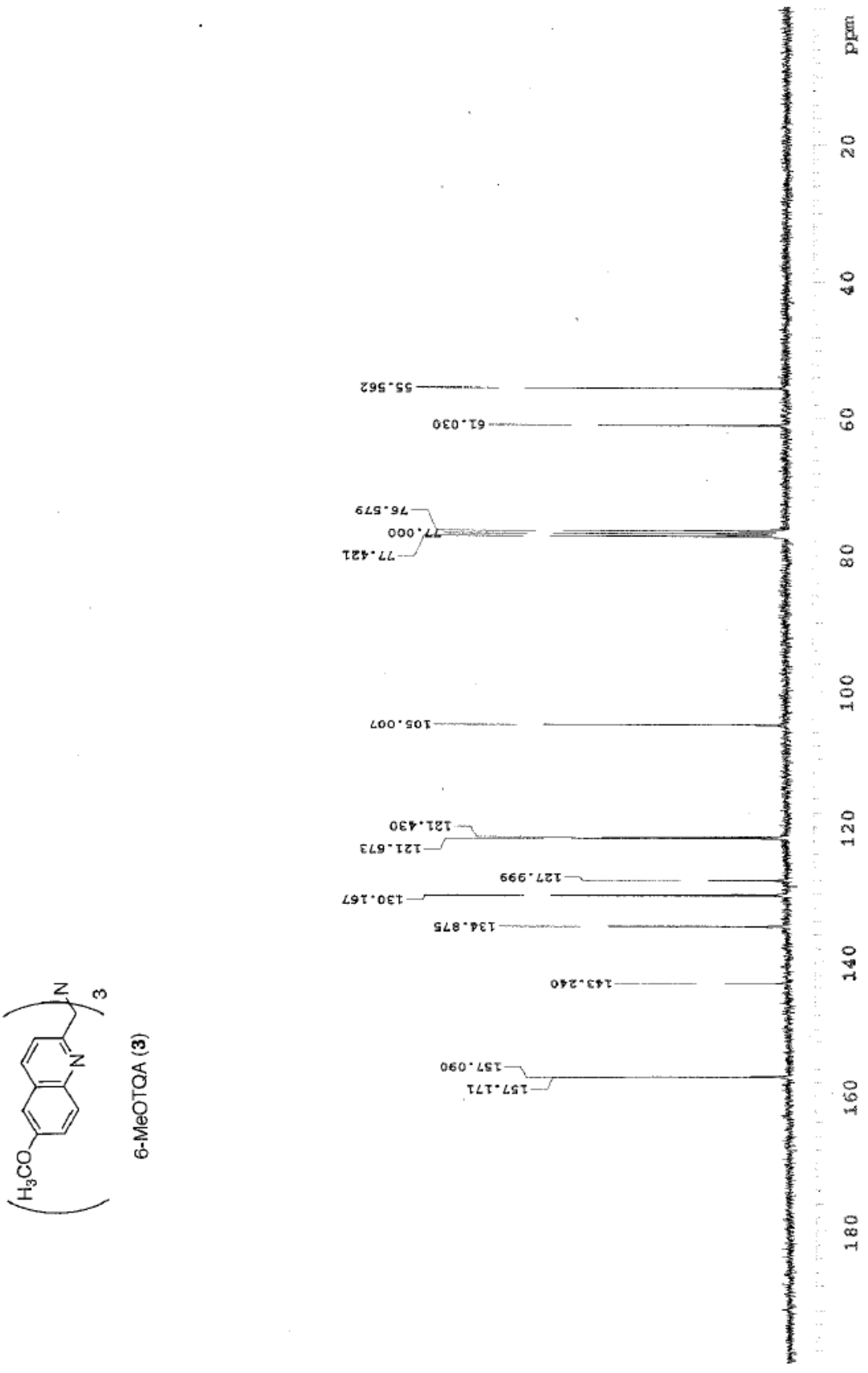

Fig. S14 ^{13}C NMR spectrum of 6-MeOTQA (**3**) in $CDCl_3$.

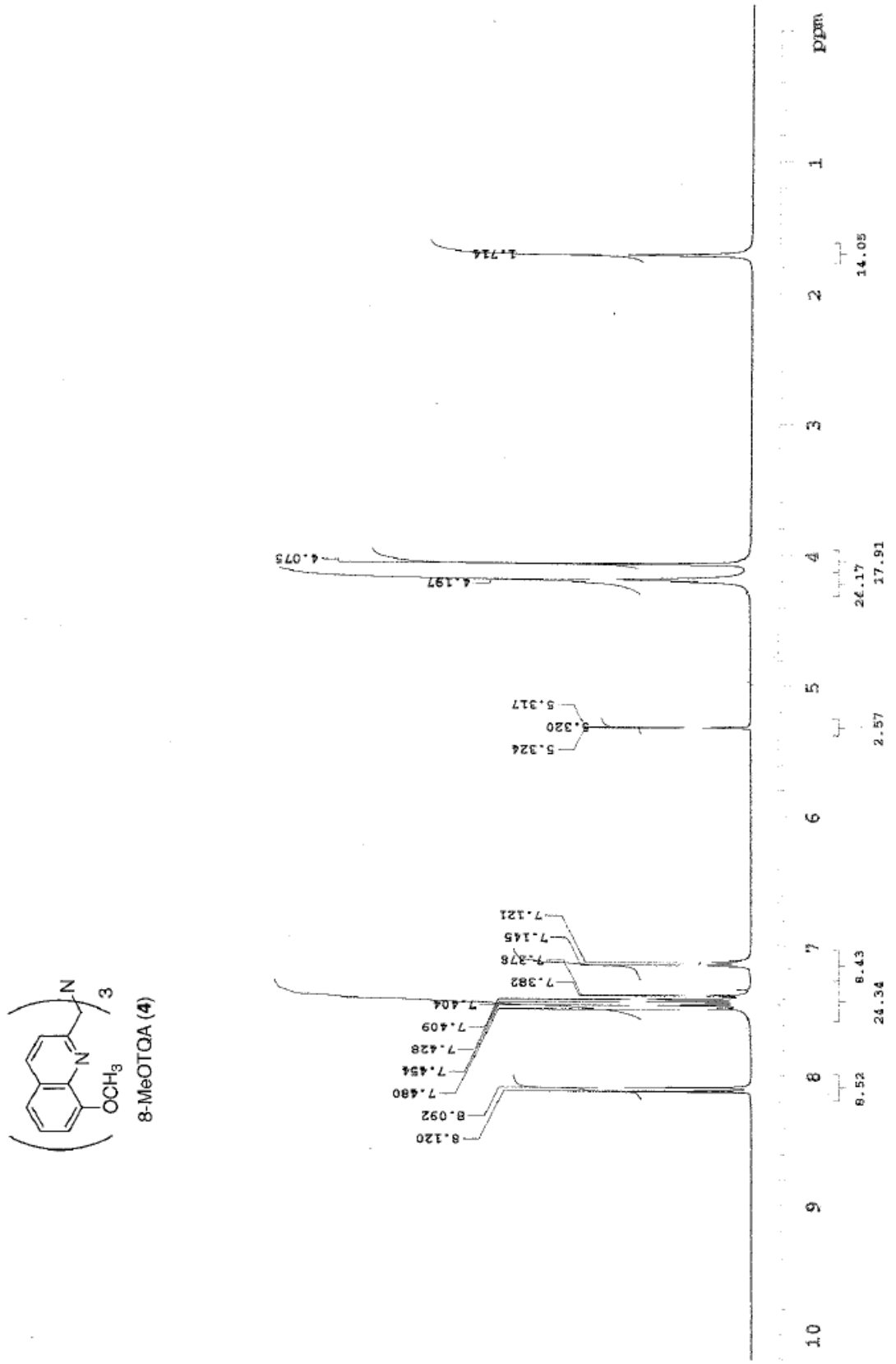

Fig. S15 ^{1}H NMR spectrum of 8-MeOTQA (**4**) in CD_2Cl_2.

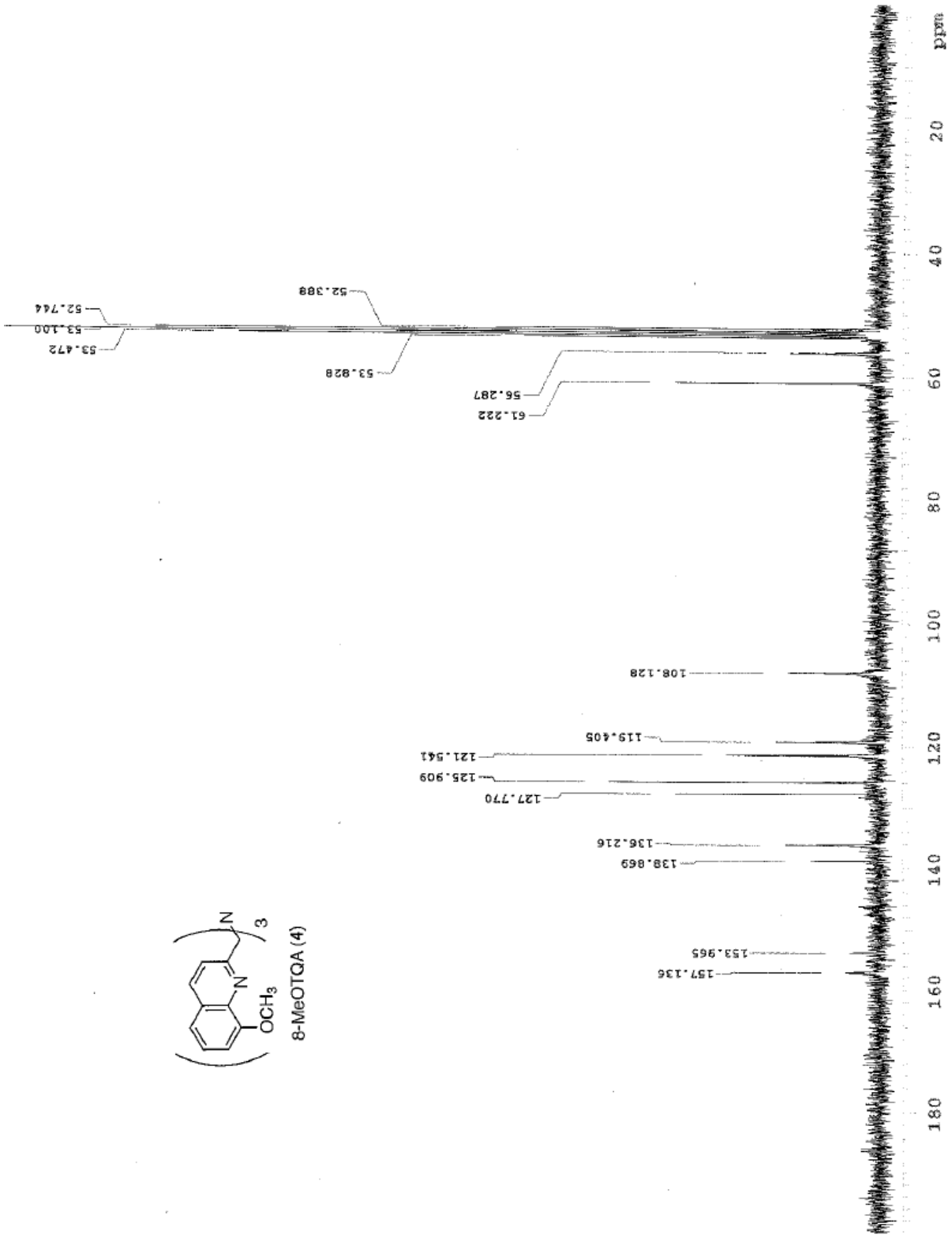

Fig. S16 ^{13}C NMR spectrum of 8-MeOTQA (**4**) in CD_2Cl_2.

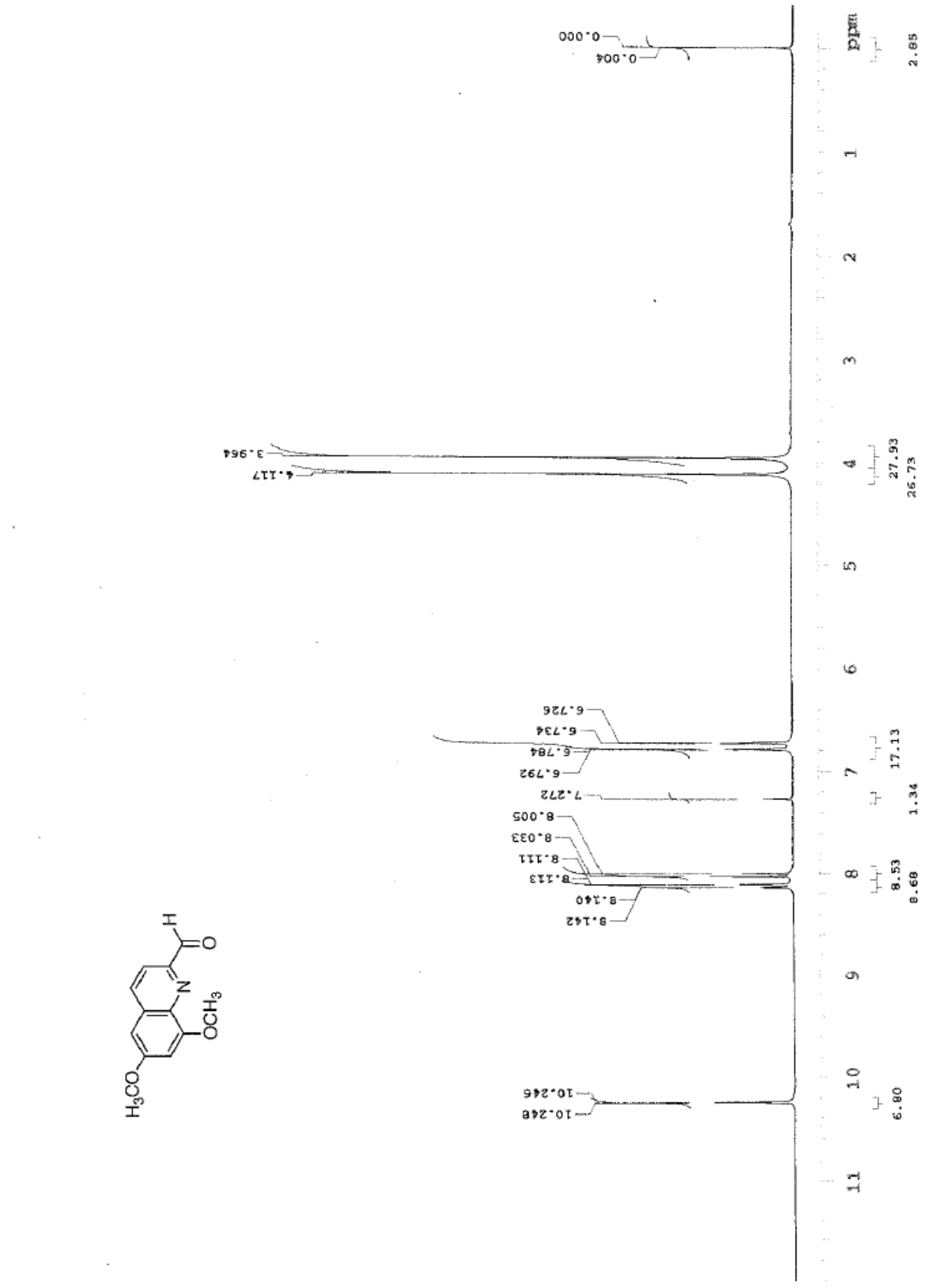

Fig. S17 ^{1}H NMR spectrum of 6,8-dimethoxy-2-quinolinecarbaldehyde in $CDCl_3$.

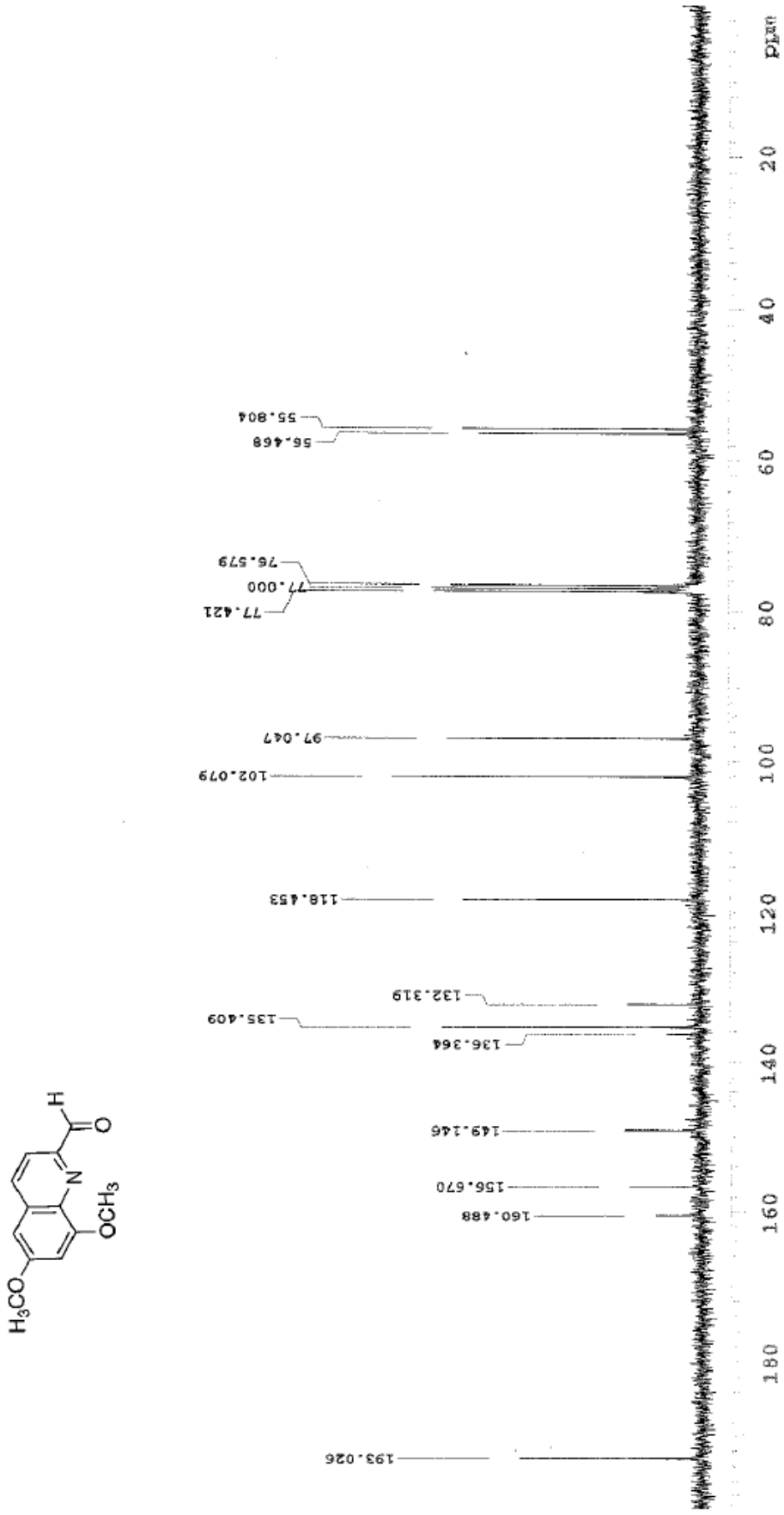

Fig. S18 ^{13}C NMR spectrum of 6,8-dimethoxy-2-quinolinecarbaldehyde in $CDCl_3$.

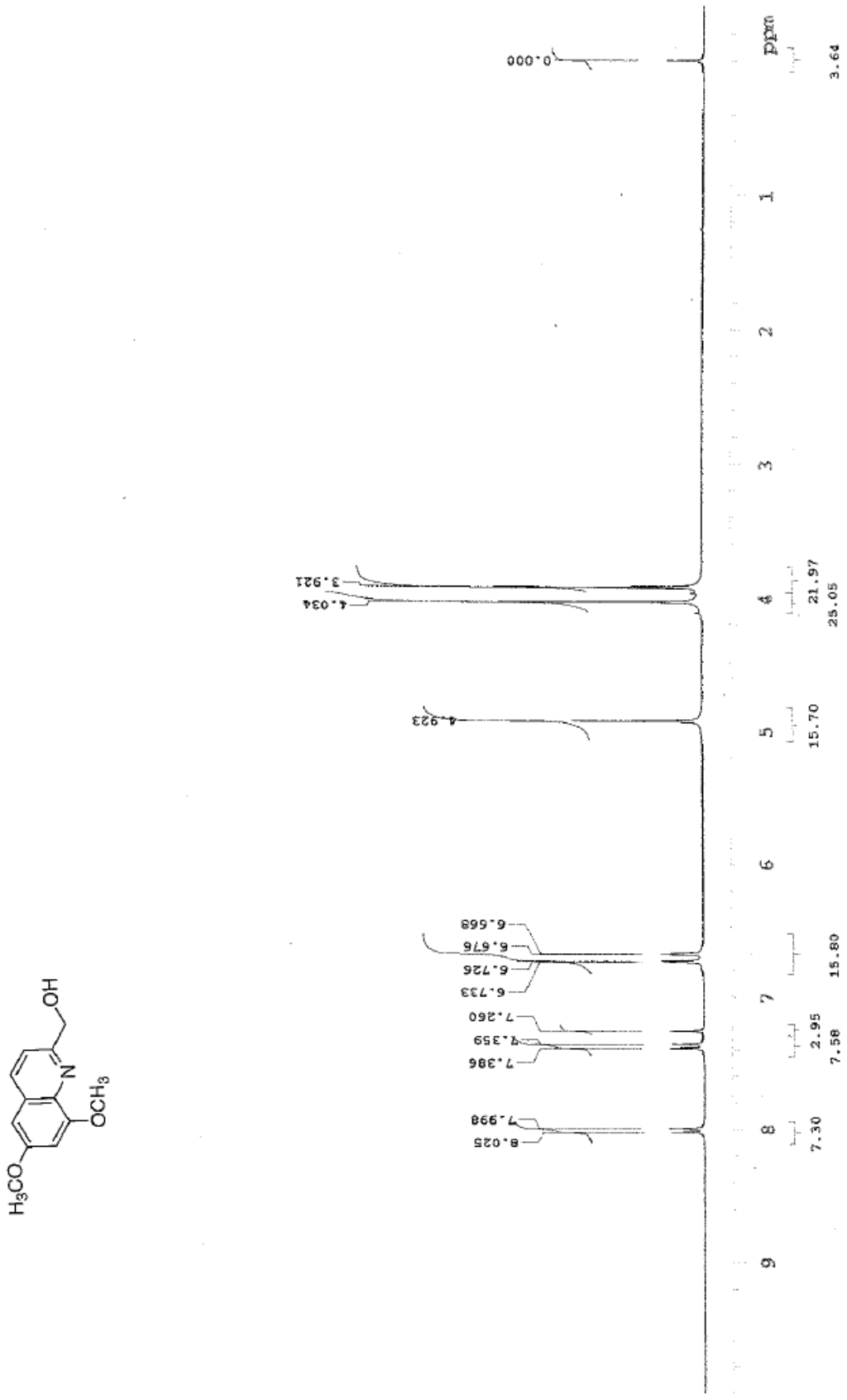

Fig. S19 ^{1}H NMR spectrum of 6,8-dimethoxy-2-hydroxymethylquinoline in $CDCl_3$.

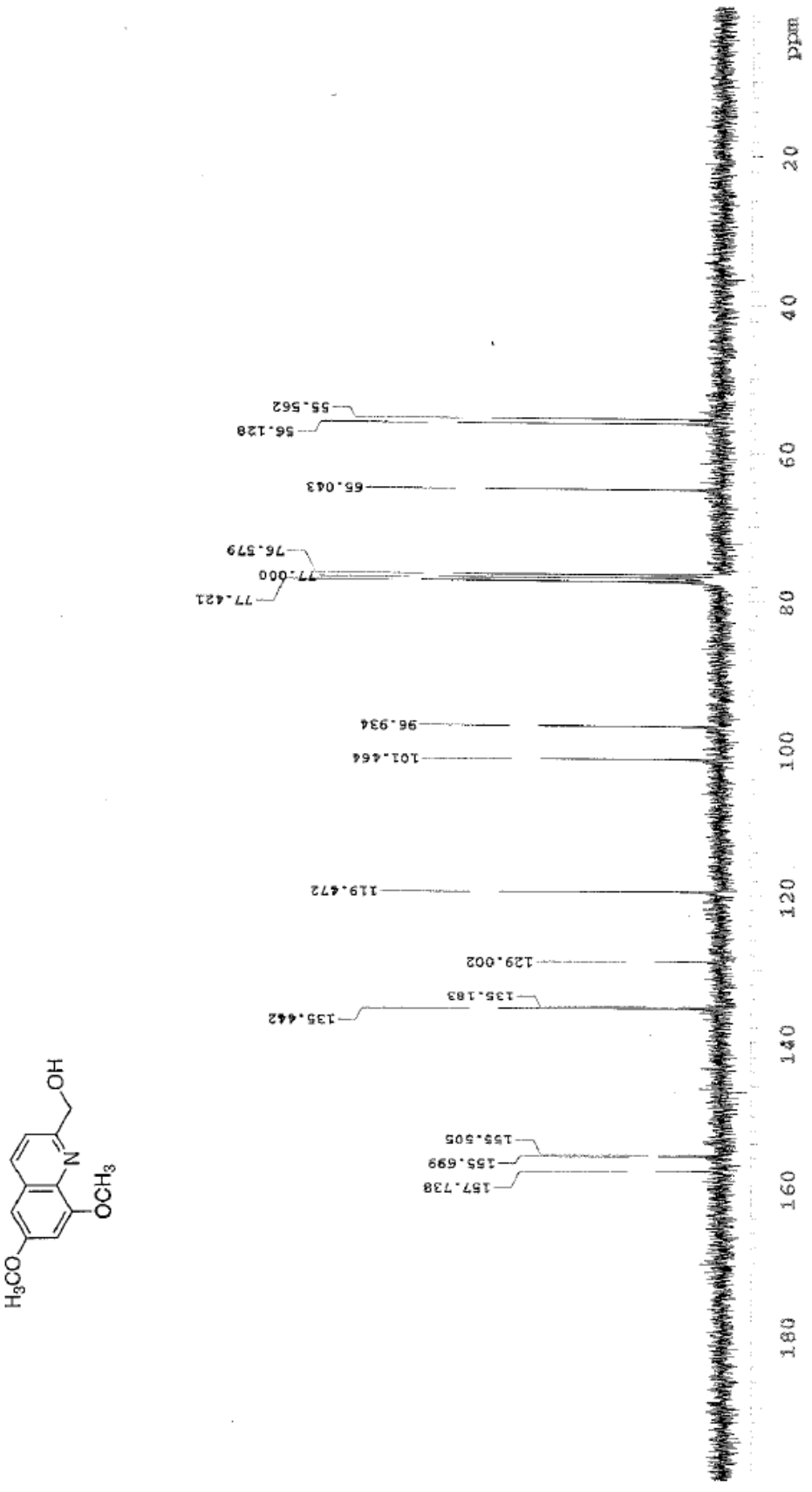

Fig. S20 ^{13}C NMR spectrum of 6,8-dimethoxy-2-hydroxymethylquinoline in $CDCl_3$.

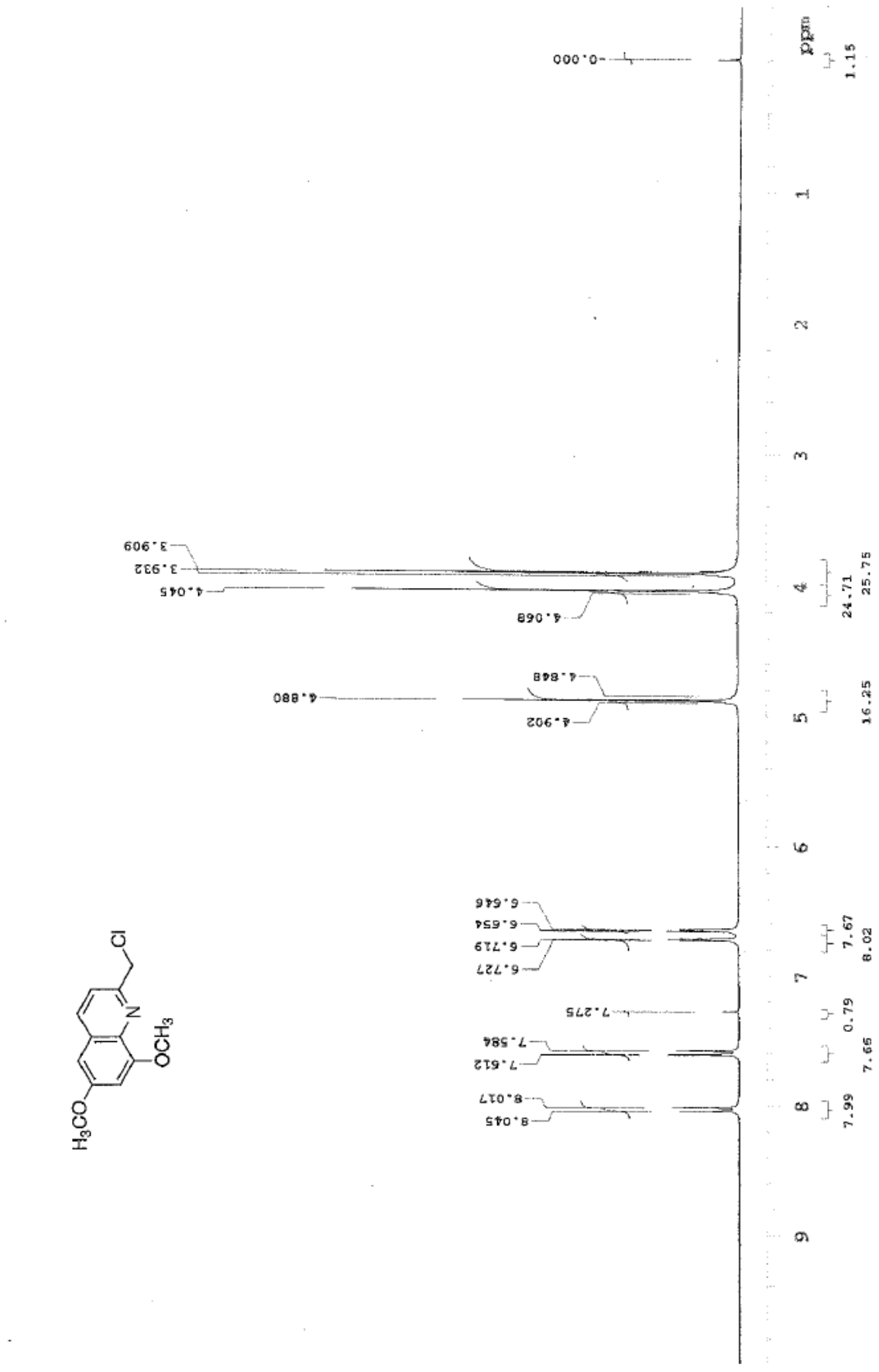

Fig. S21 ^{1}H NMR spectrum of 6,8-dimethoxy-2-chloromethylquinoline in $CDCl_3$.

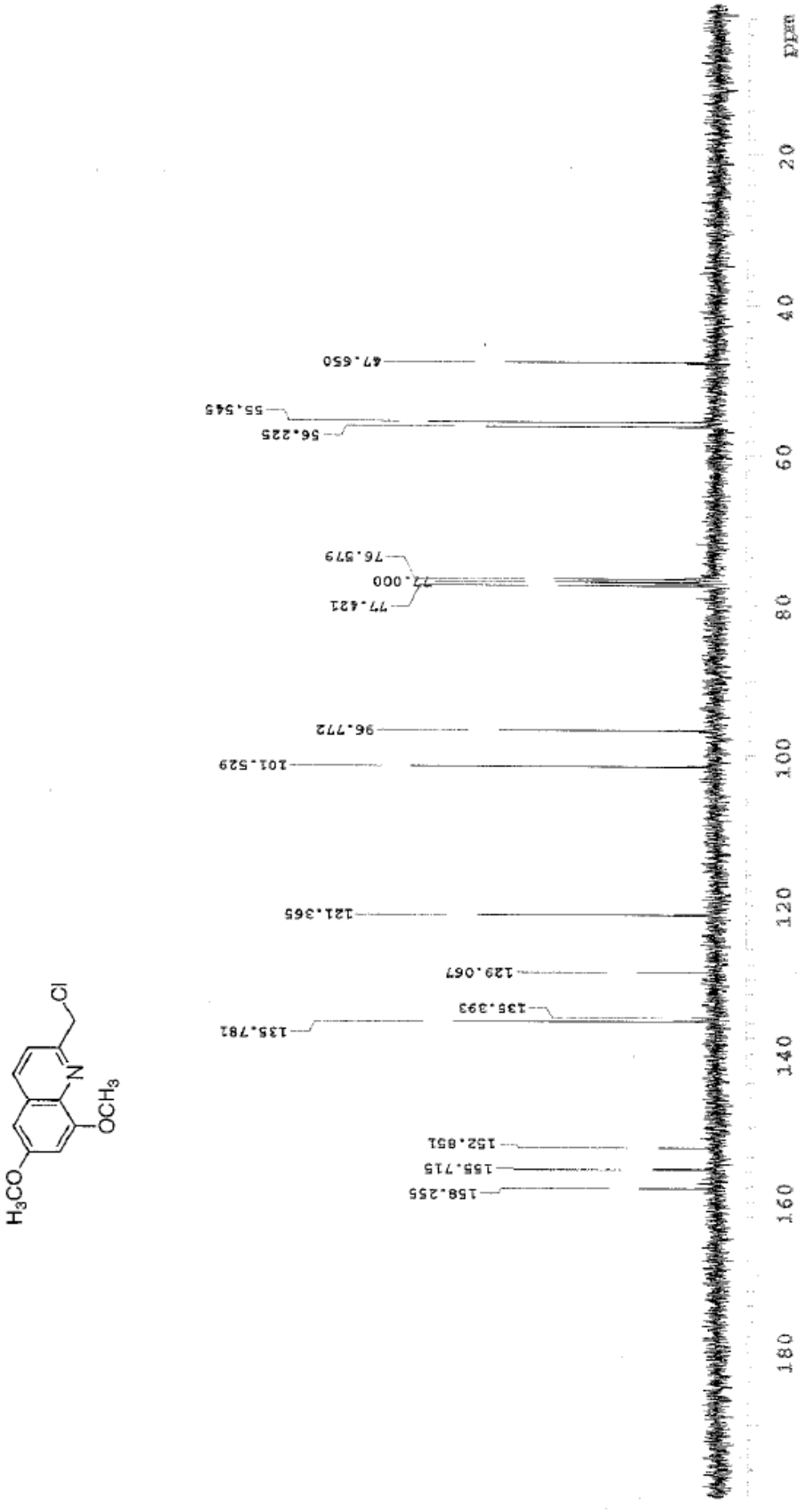

Fig. S22 ^{13}C NMR spectrum of 6,8-dimethoxy-2-chloromethylquinoline in $CDCl_3$.

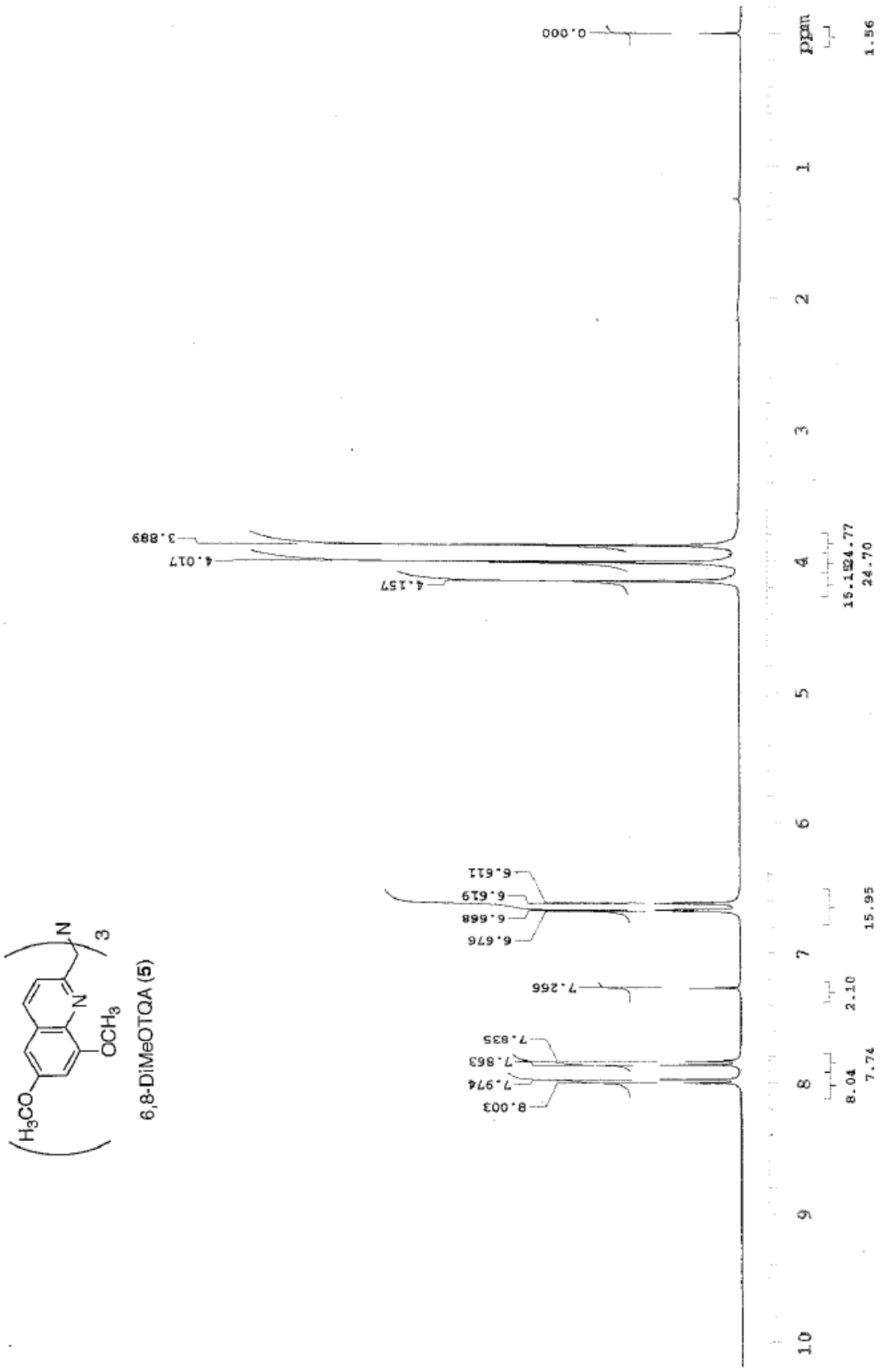

Fig. S23 ^{1}H NMR spectrum of 6,8-DiMeOTQA (**5**) in $CDCl_3$.

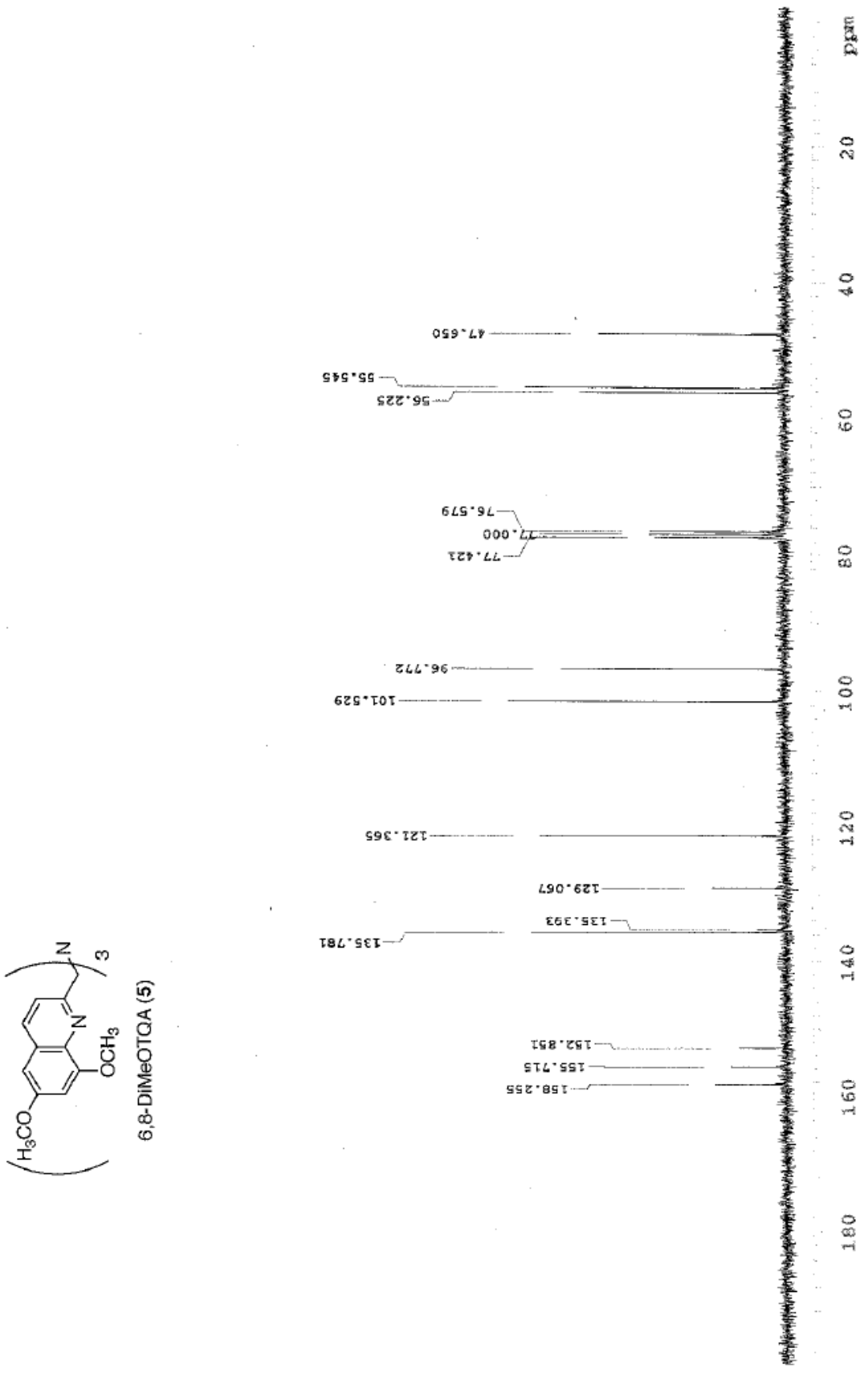

Fig. S24 ^{13}C NMR spectrum of 6,8-DiMeOTQA (**5**) in $CDCl_3$.

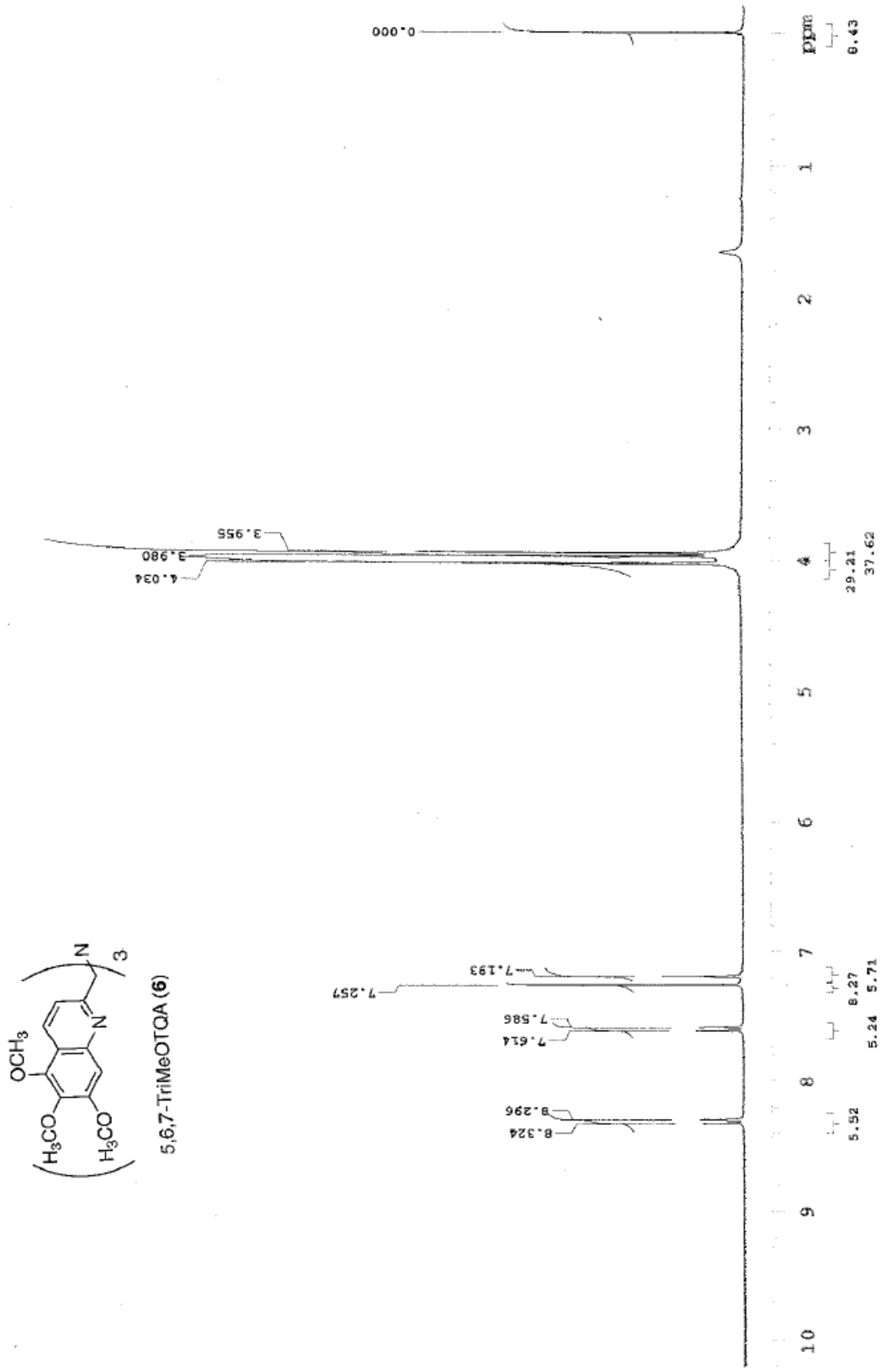

Fig. S25 ^{1}H NMR spectrum of 5,6,7-TriMeOTQA (**6**) in $CDCl_3$.

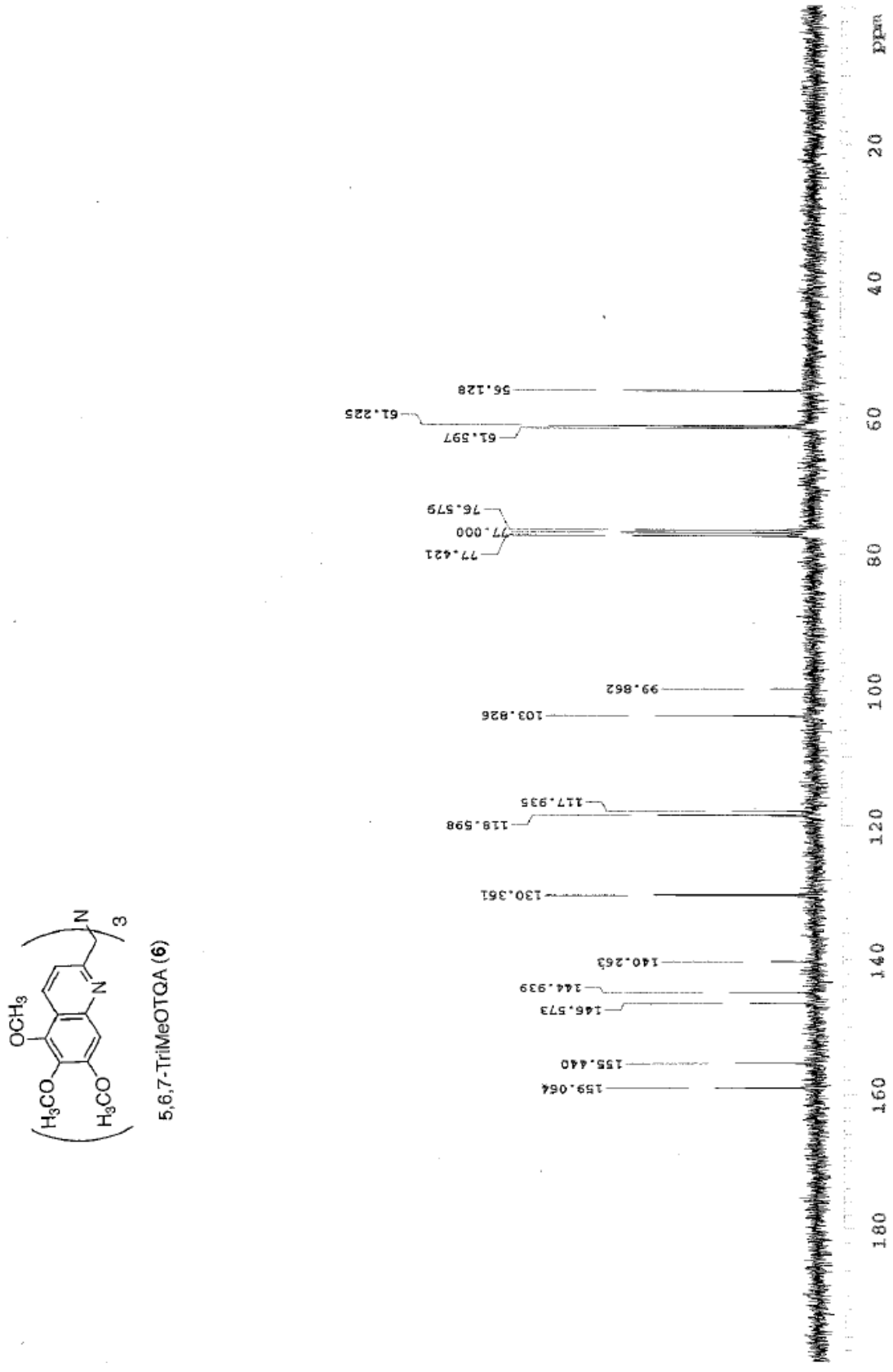

Fig. S26 ^{13}C NMR spectrum of 5,6,7-TriMeOTQA (**6**) in $CDCl_3$.

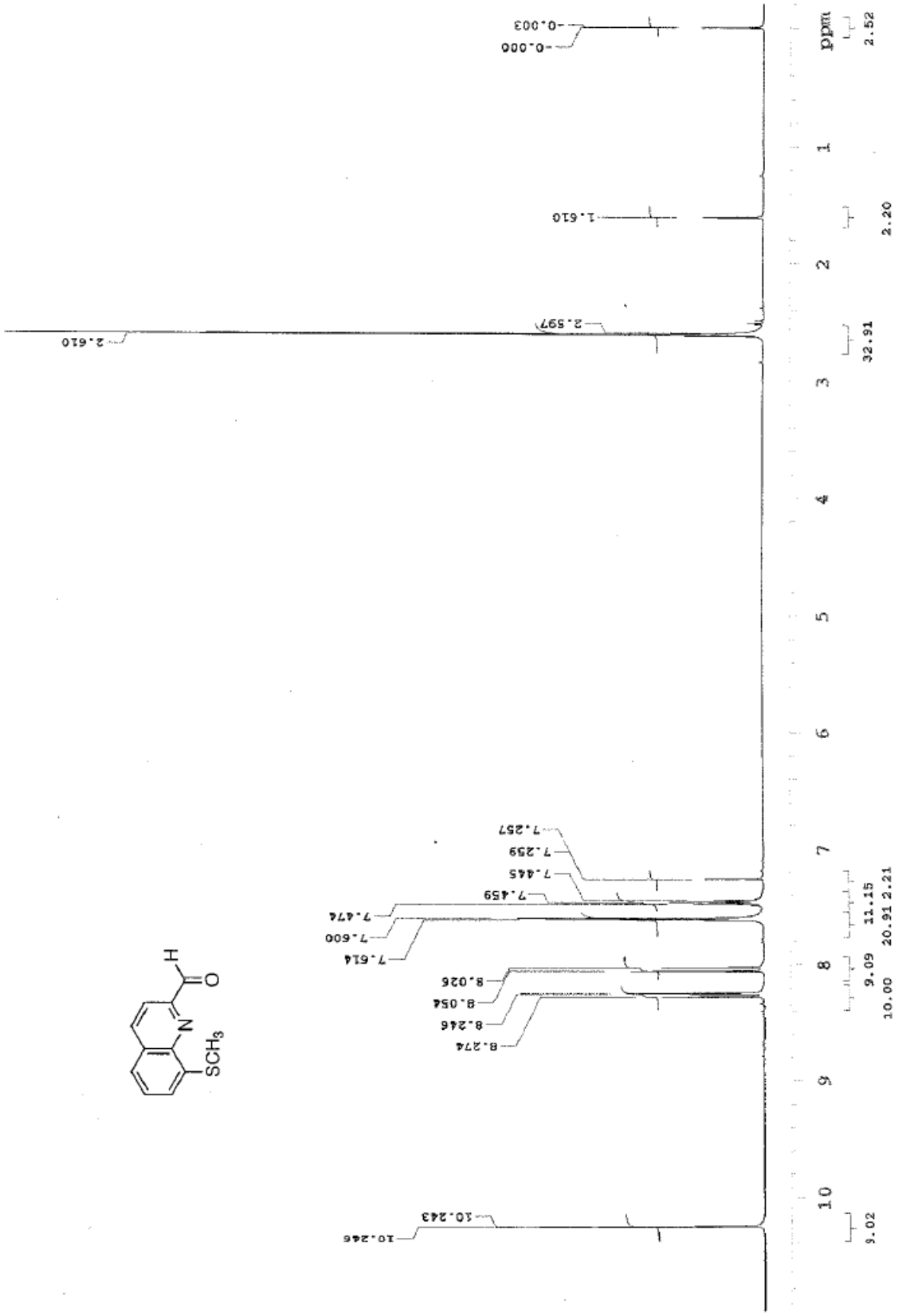

Fig. S27 ^{1}H NMR spectrum of 8-methylthioquinoline-2-carbaldehyde in $CDCl_3$.

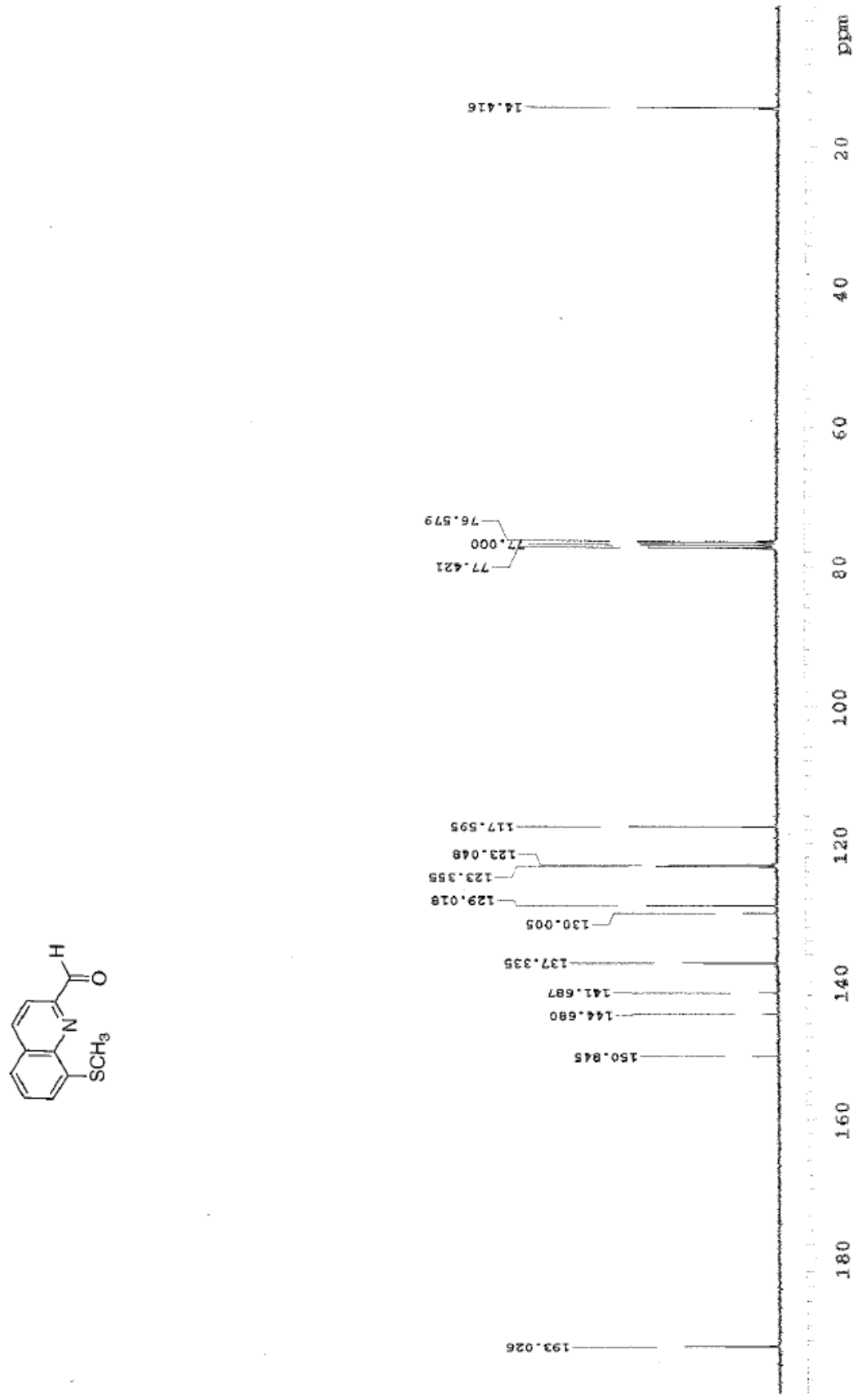

Fig. S28 ^{13}C NMR spectrum of 8-methylthioquinoline-2-carbaldehyde in $CDCl_3$.

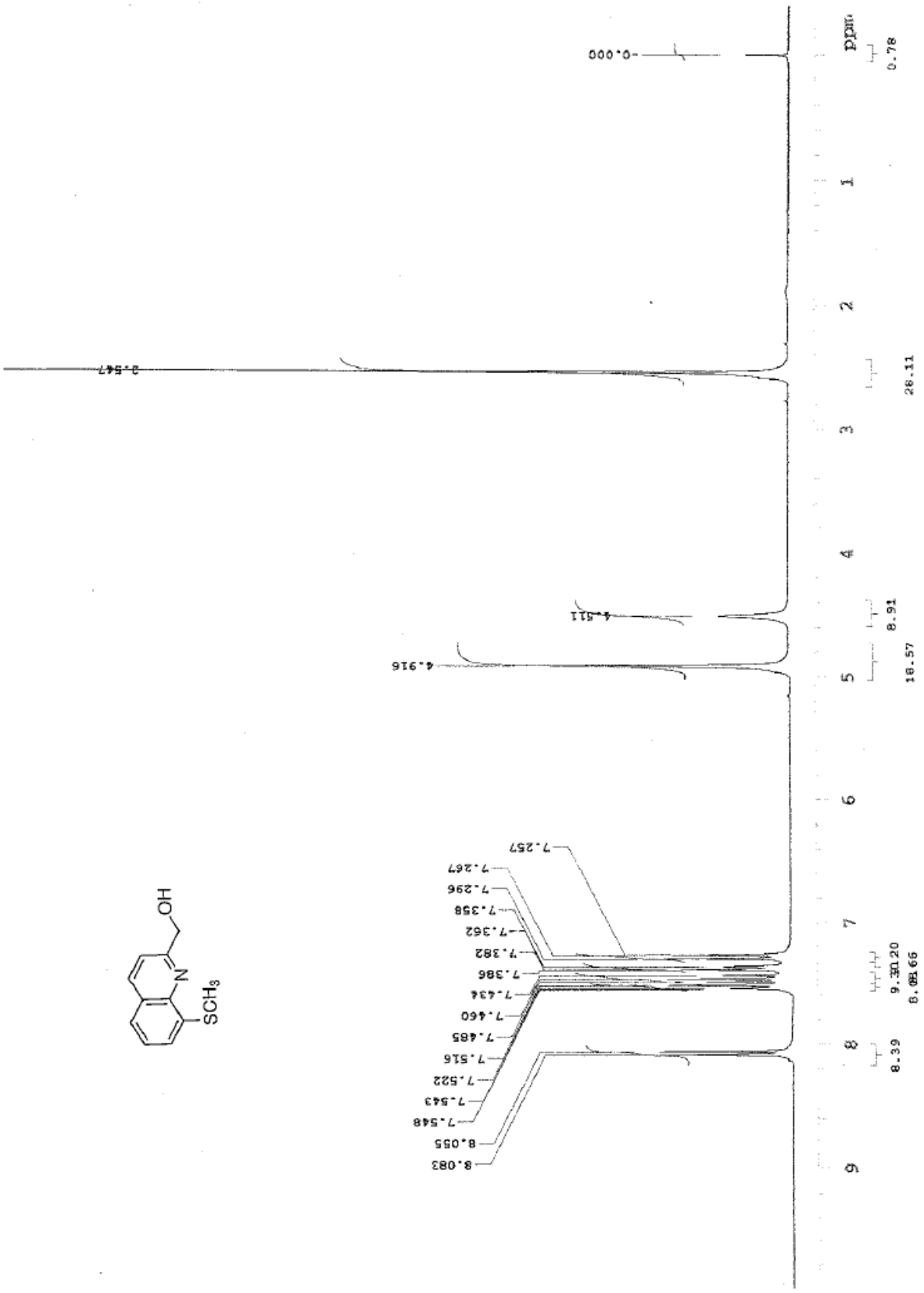

Fig. S29 ^{1}H NMR spectrum of 8-methylthio-2-hydroxymethylquinoline in $CDCl_3$.

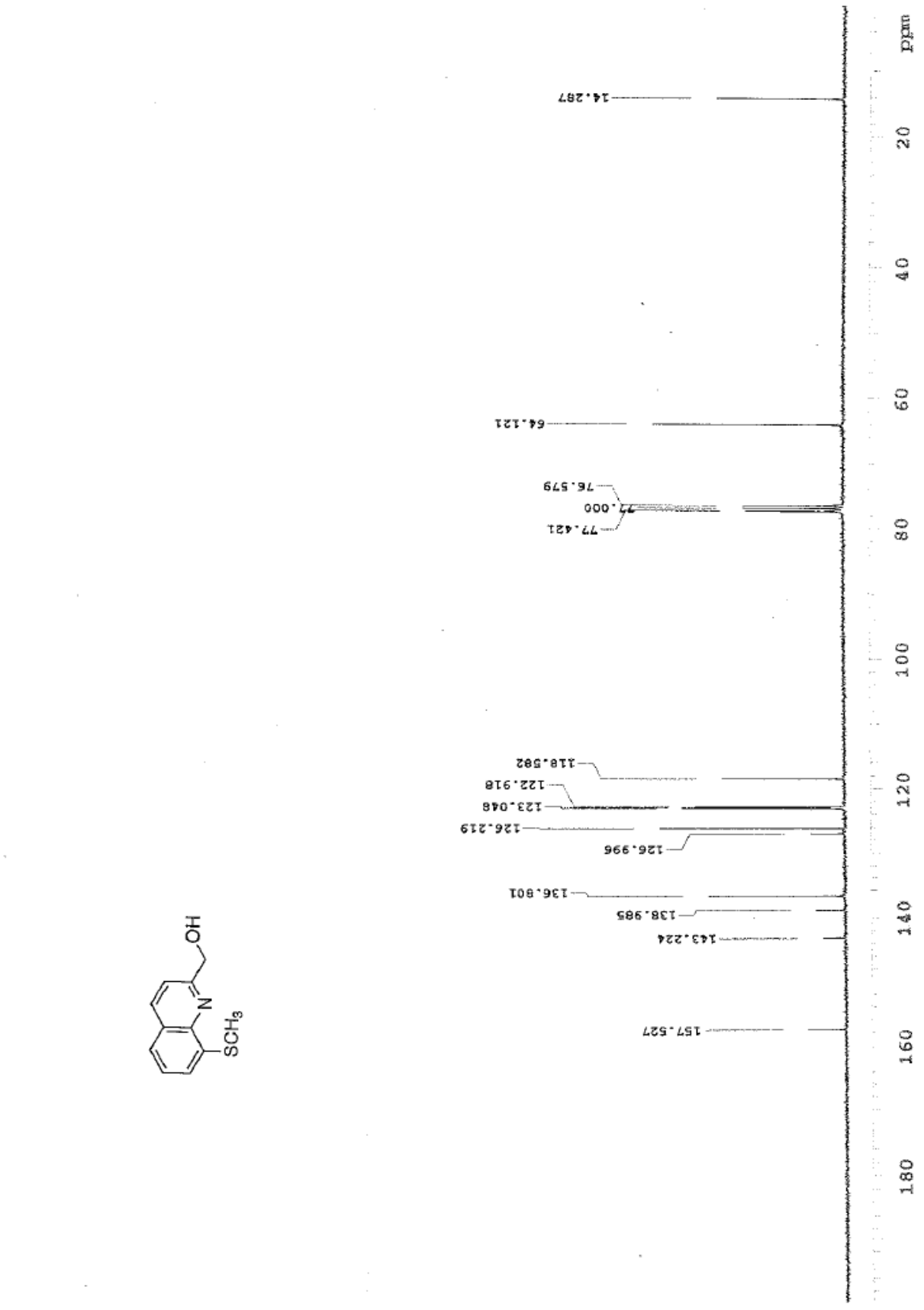

Fig. S30 ^{13}C NMR spectrum of 8-methylthio-2-hydroxymethylquinoline in $CDCl_3$.

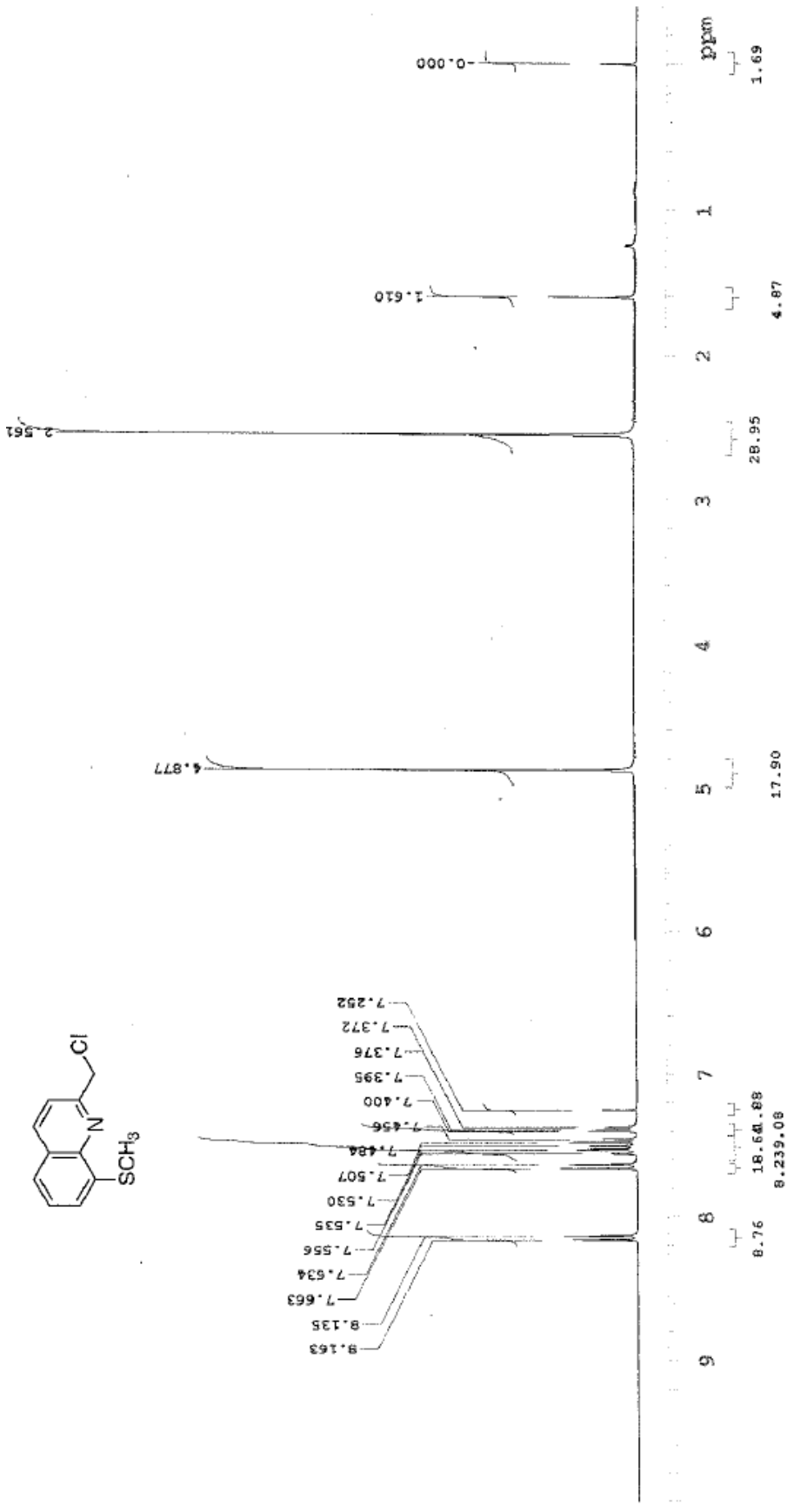

Fig. S31 ^{1}H NMR spectrum of 8-methylthio-2-chloromethylquinoline in $CDCl_3$.

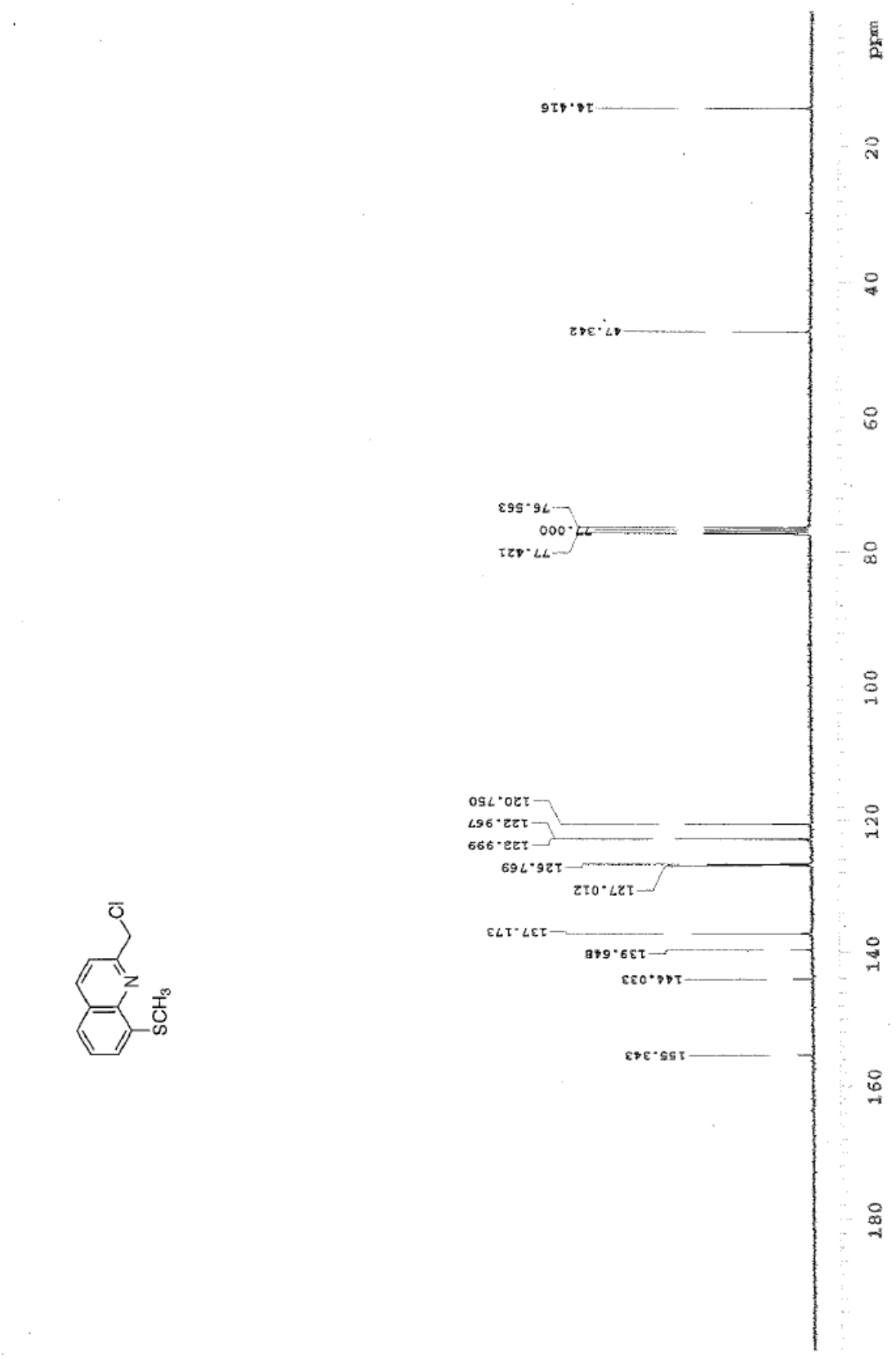

Fig. S32 ^{13}C NMR spectrum of 8-methylthio-2-chloromethylquinoline in $CDCl_3$.

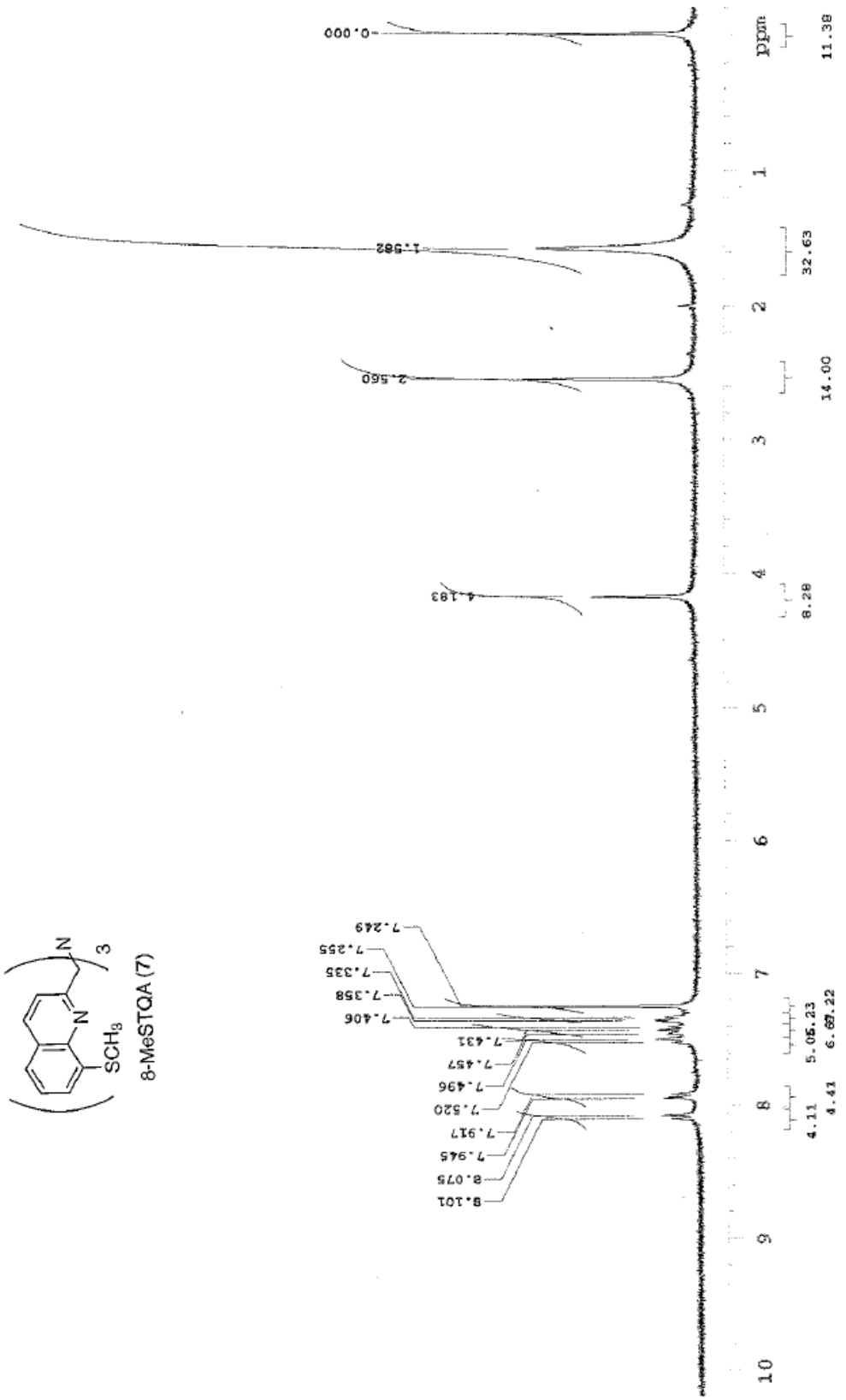

Fig. S33 ^{1}H NMR spectrum of 8-MeSTQA (**7**) in $CDCl_3$.

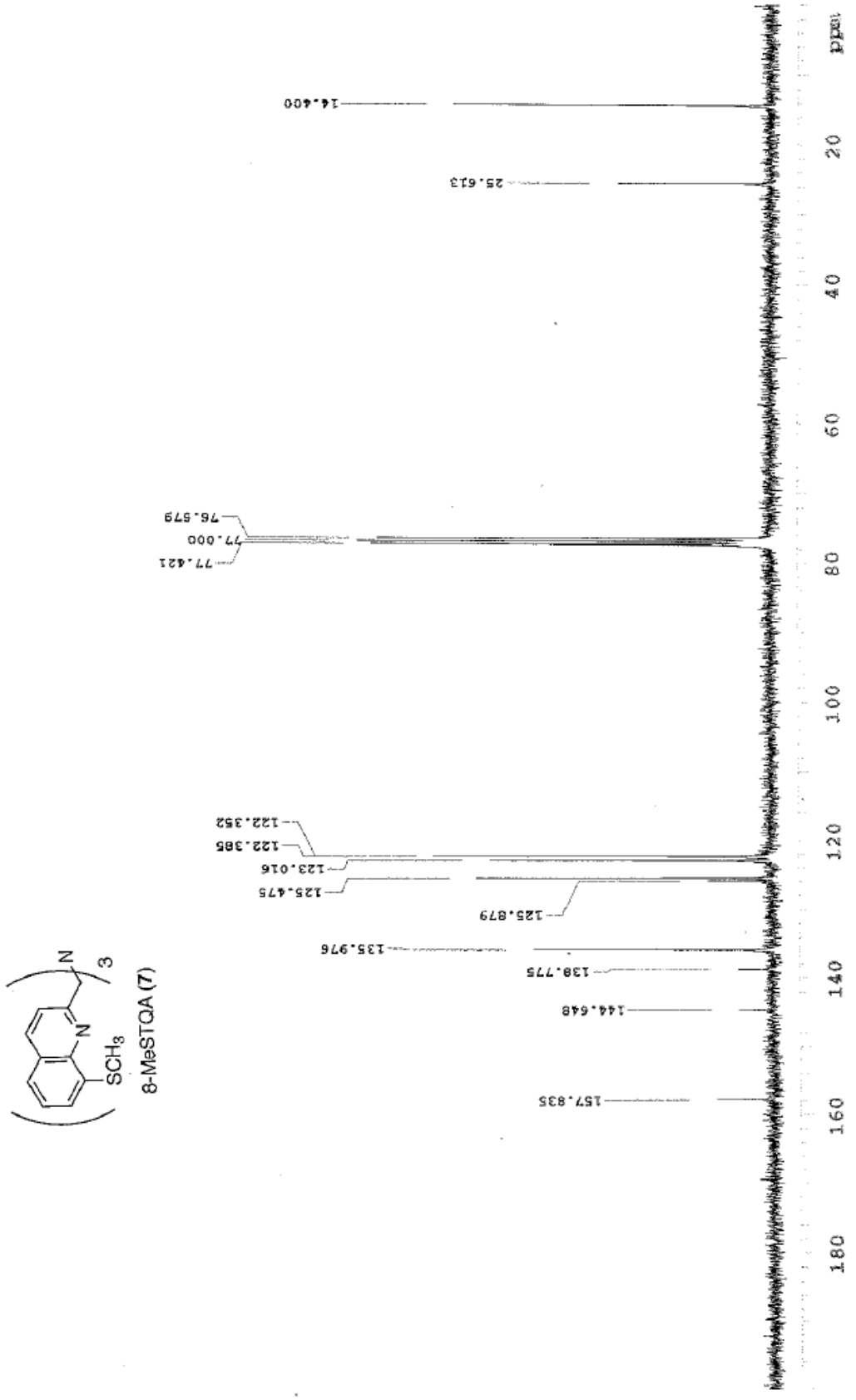

Fig. S34 ^{13}C NMR spectrum of 8-MeSTQA (**7**) in $CDCl_3$.

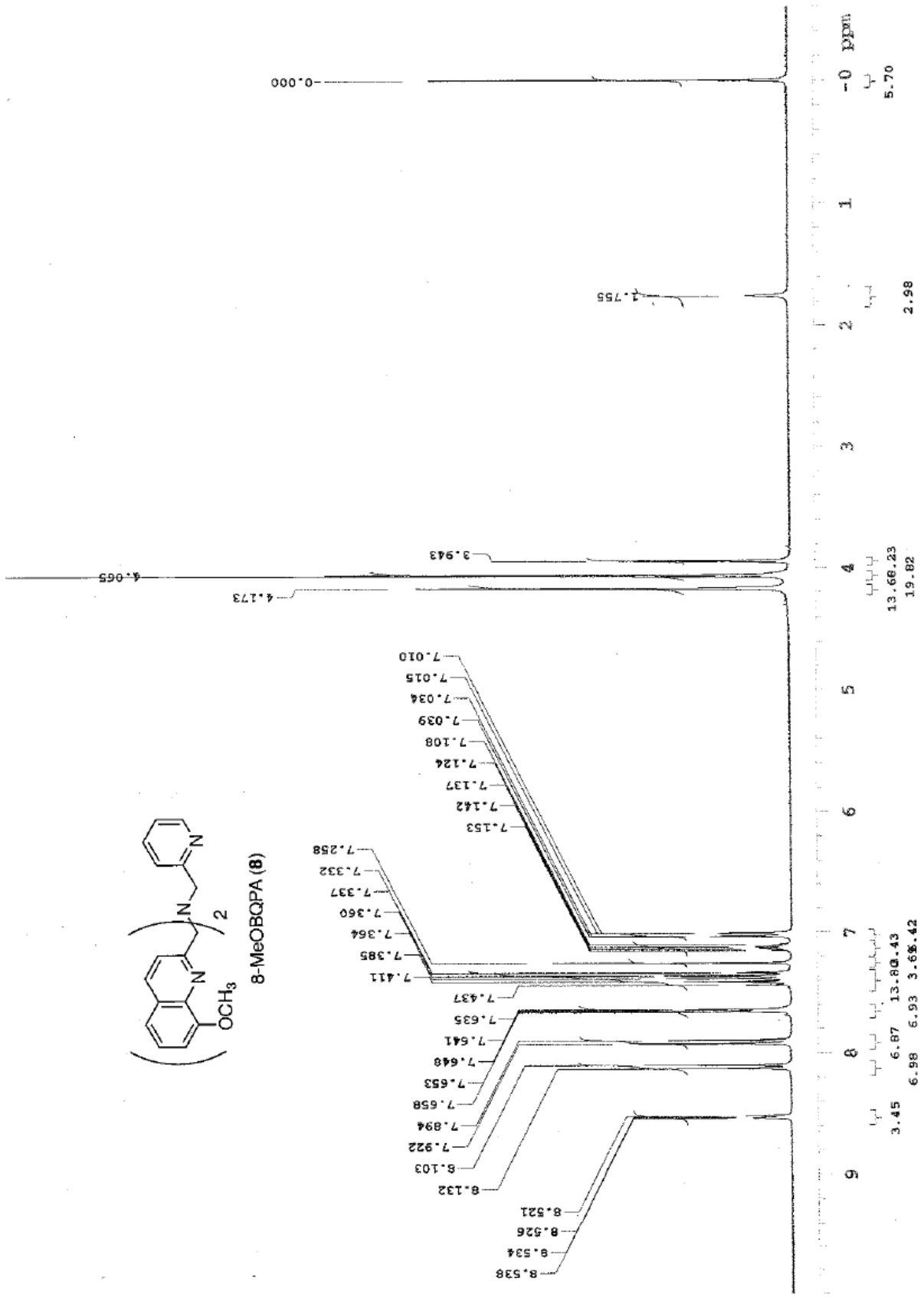

Fig. S35 ^{1}H NMR spectrum of 8-MeOBQPA (**8**) in $CDCl_3$.

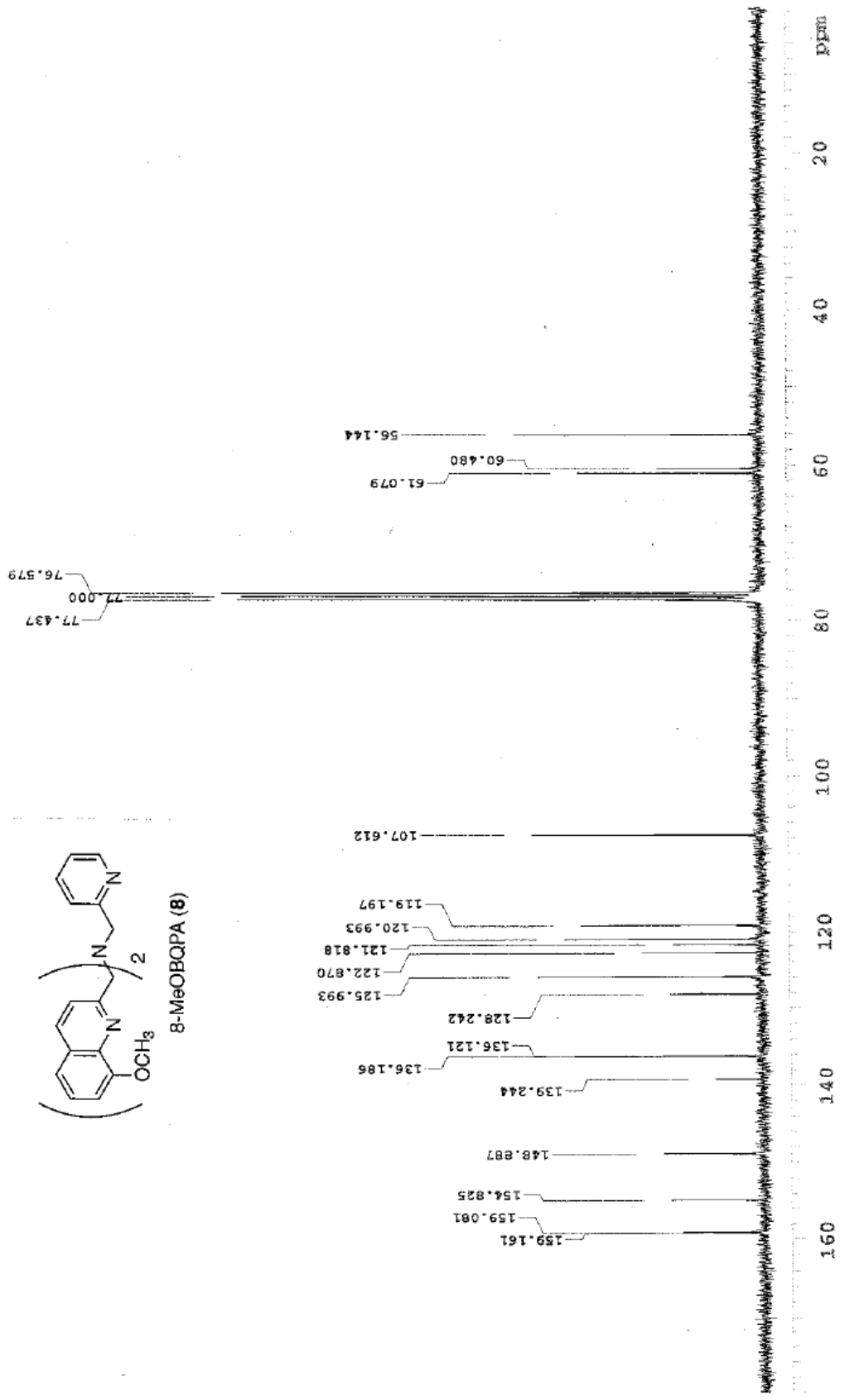

Fig. S36 ^{13}C NMR spectrum of 8-MeOBQPA (**8**) in $CDCl_3$.

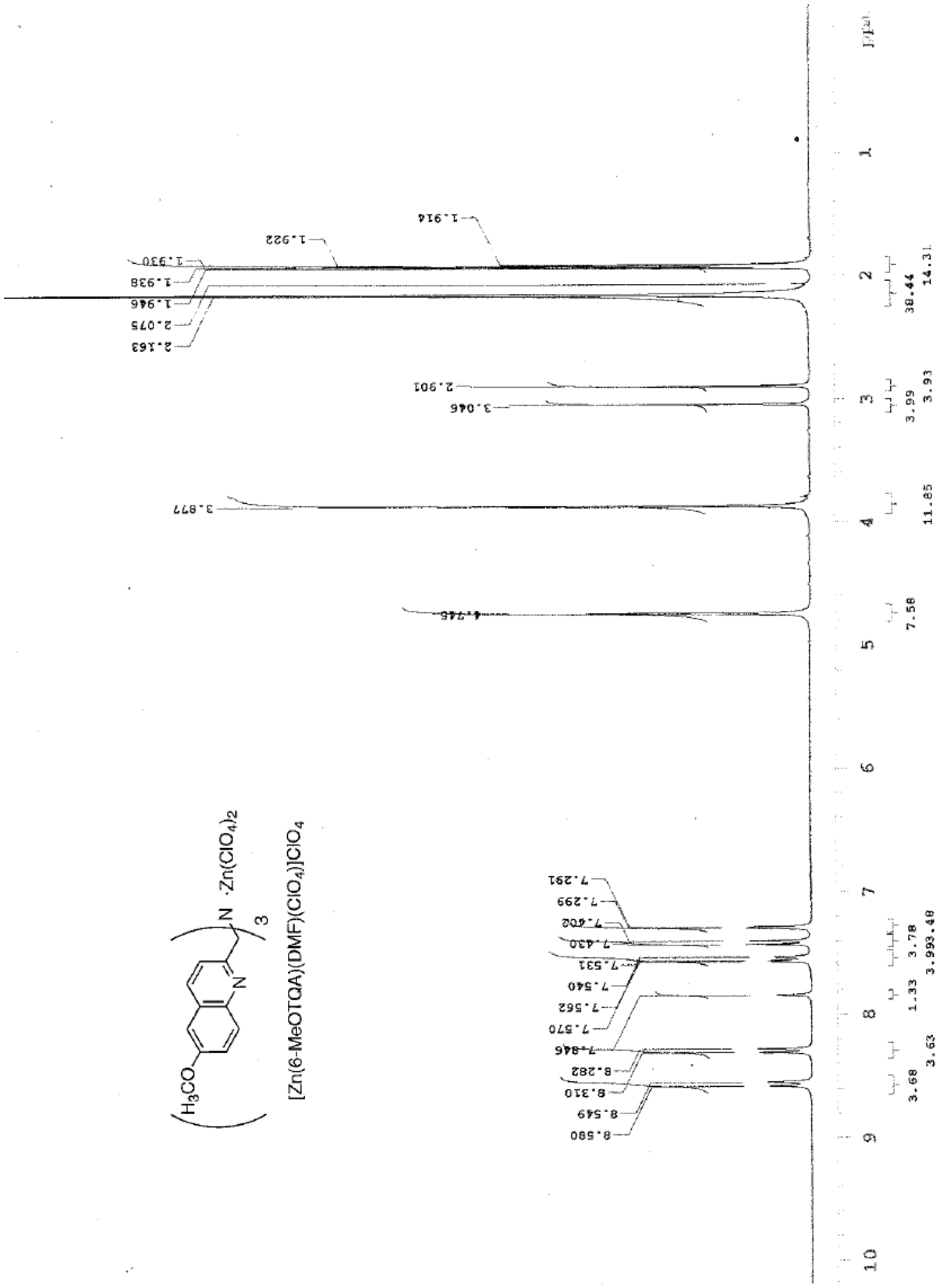

Fig. S37 ^{13}C NMR spectrum of [Zn(6-MeOTQA)(DMF)(ClO_4)]ClO_4 in CD_3CN.

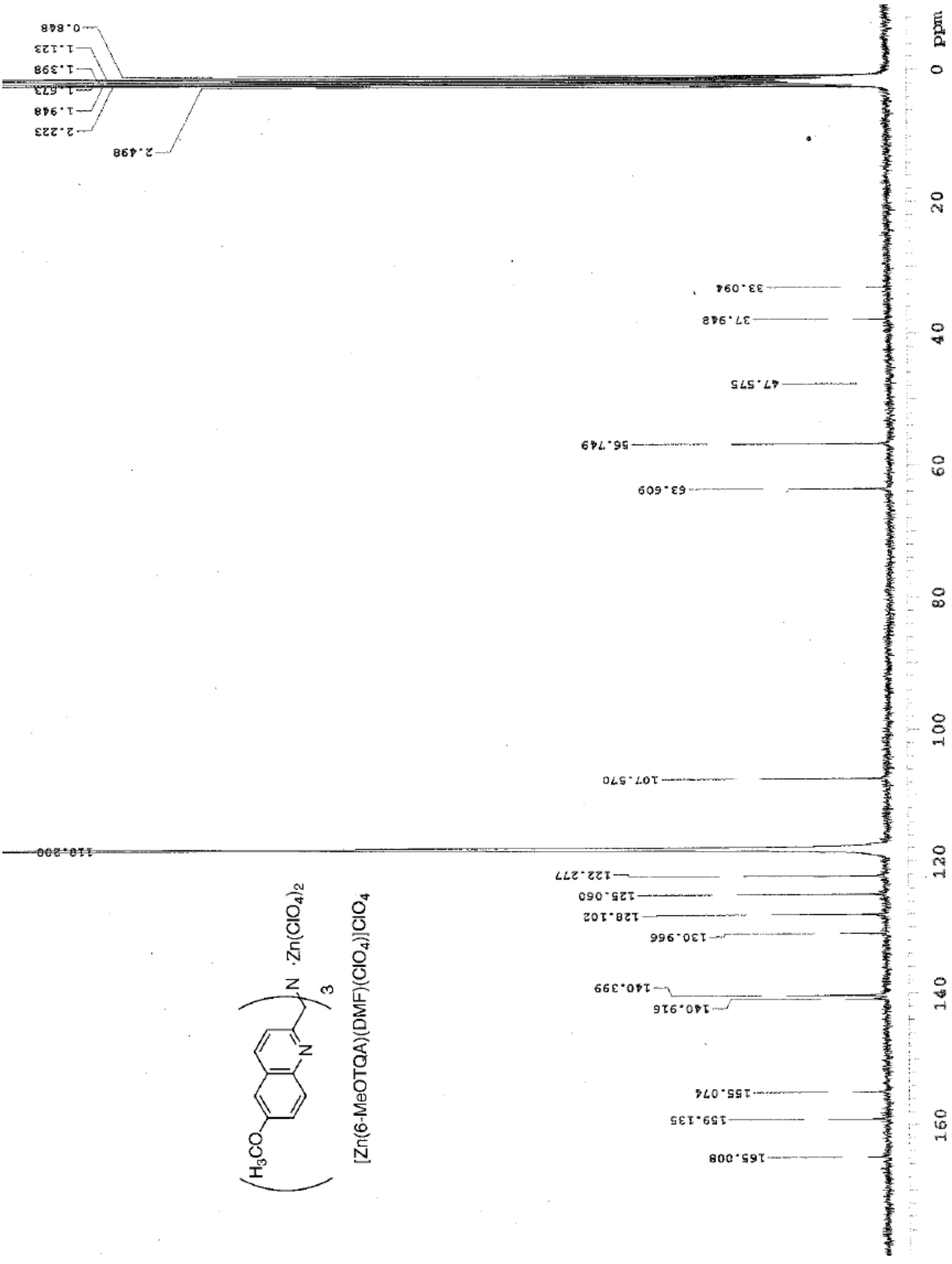

Fig. S38 ^{13}C NMR spectrum of [Zn(6-MeOTQA)(DMF)(ClO_4)]ClO_4 in CD_3CN.

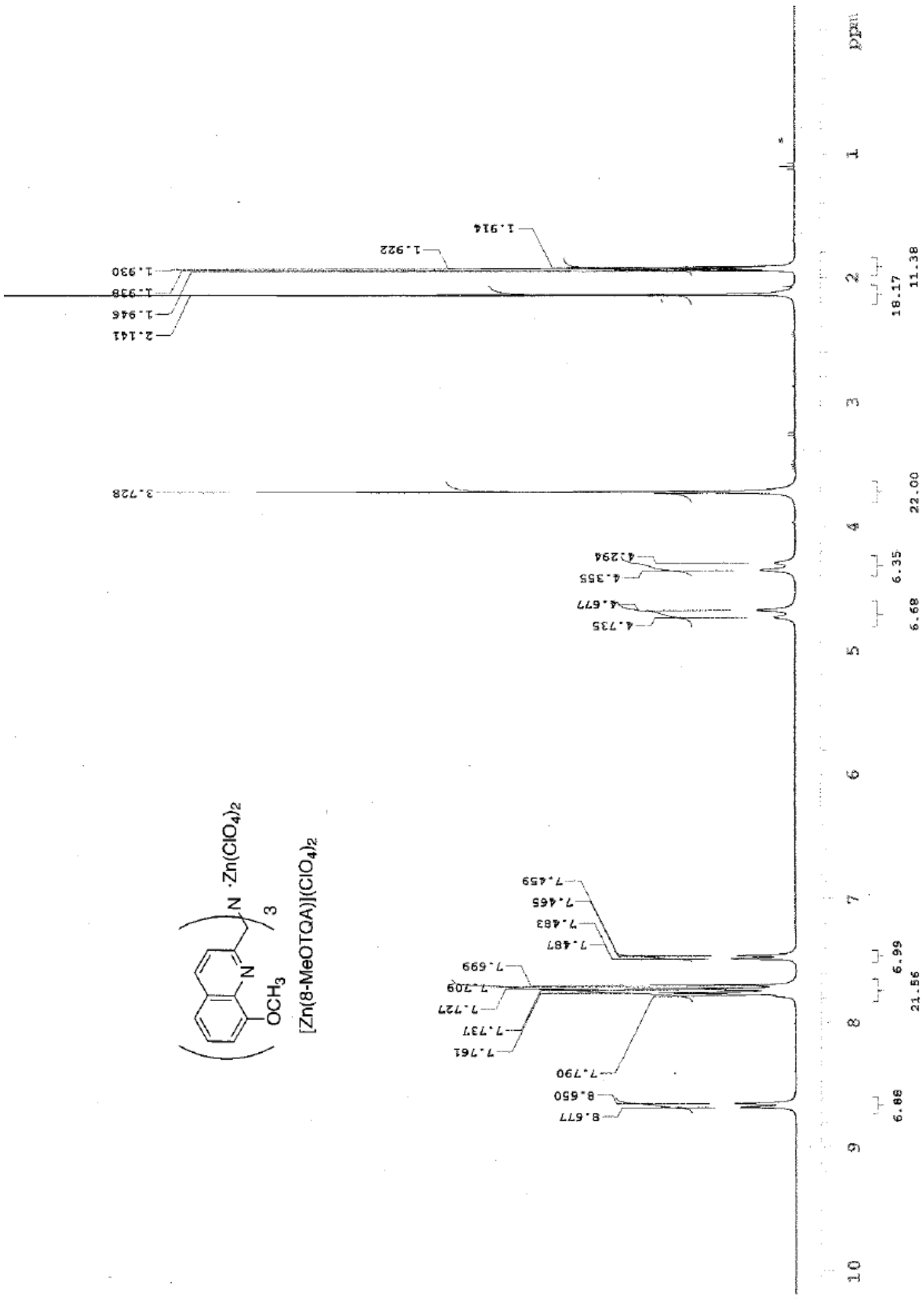

Fig. S39 ^{1}H NMR spectrum of [Zn(8-MeOTQA)](ClO$_4$)$_2$ in CD$_3$CN.

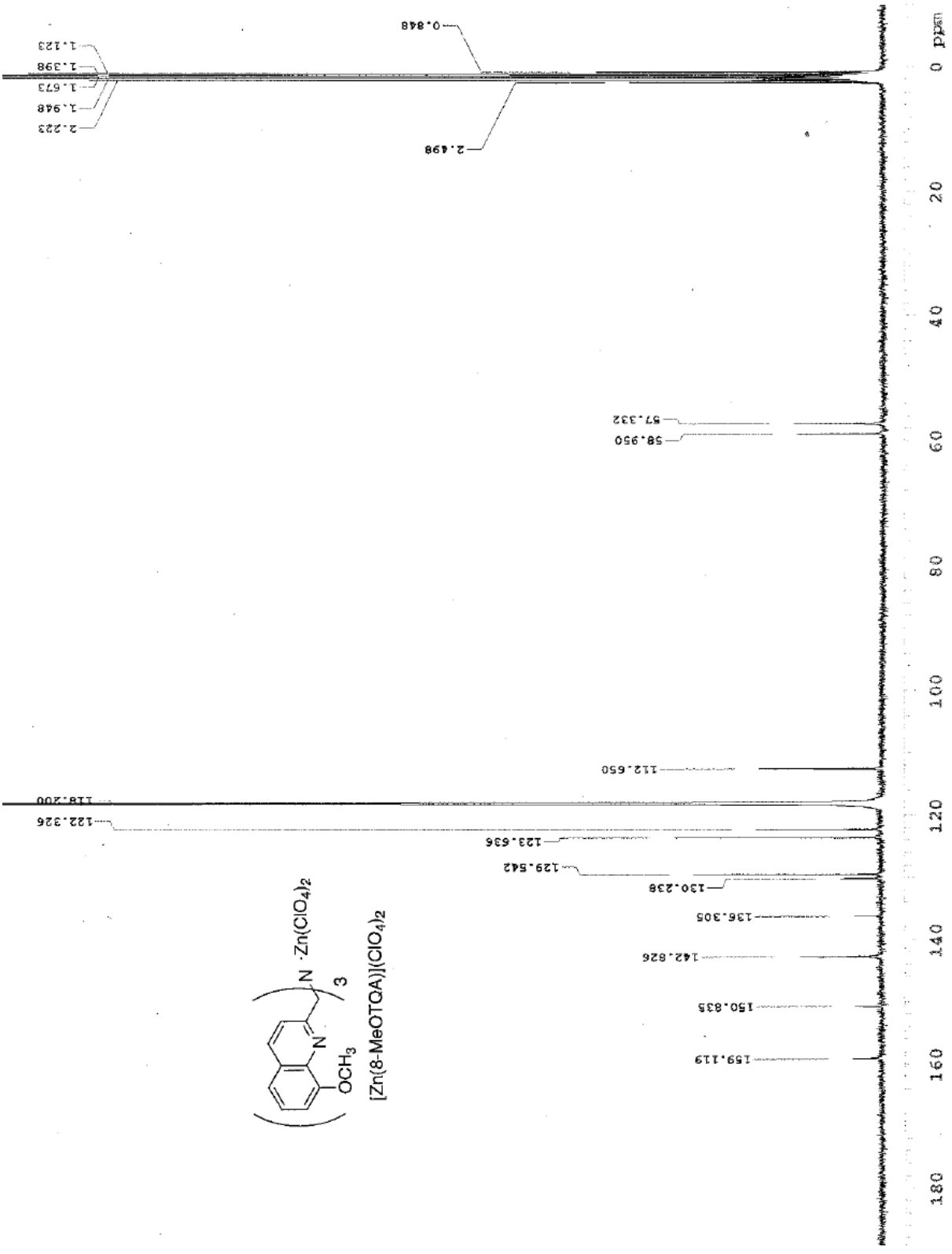

Fig. S40 ^{13}C NMR spectrum of $[Zn(8\text{-MeOTQA})](ClO_4)_2$ in CD_3CN.

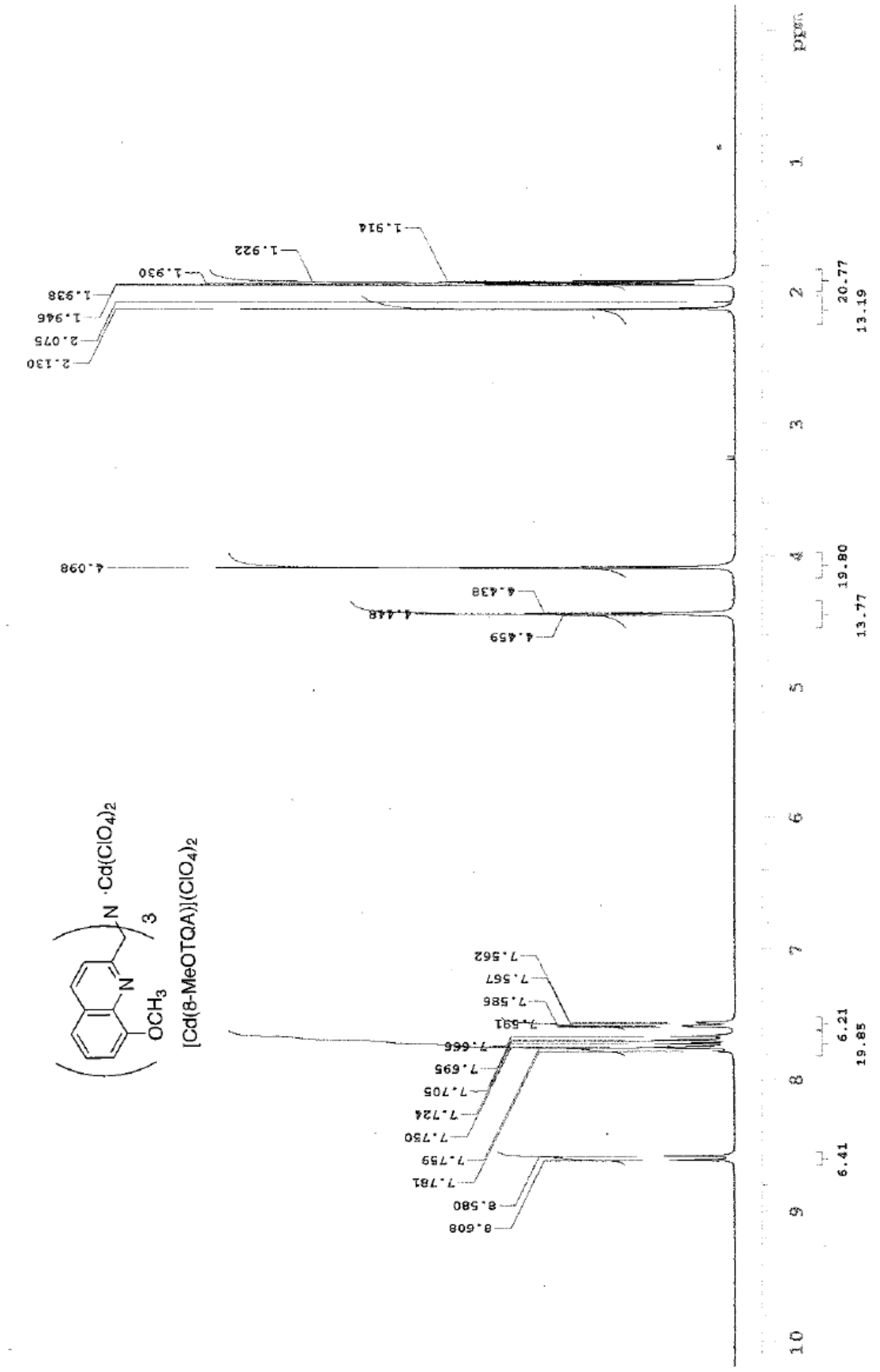

Fig. S41 ^{1}H NMR spectrum of [Cd(8-MeOTQA)](ClO$_4$)$_2$ in CD$_3$CN.

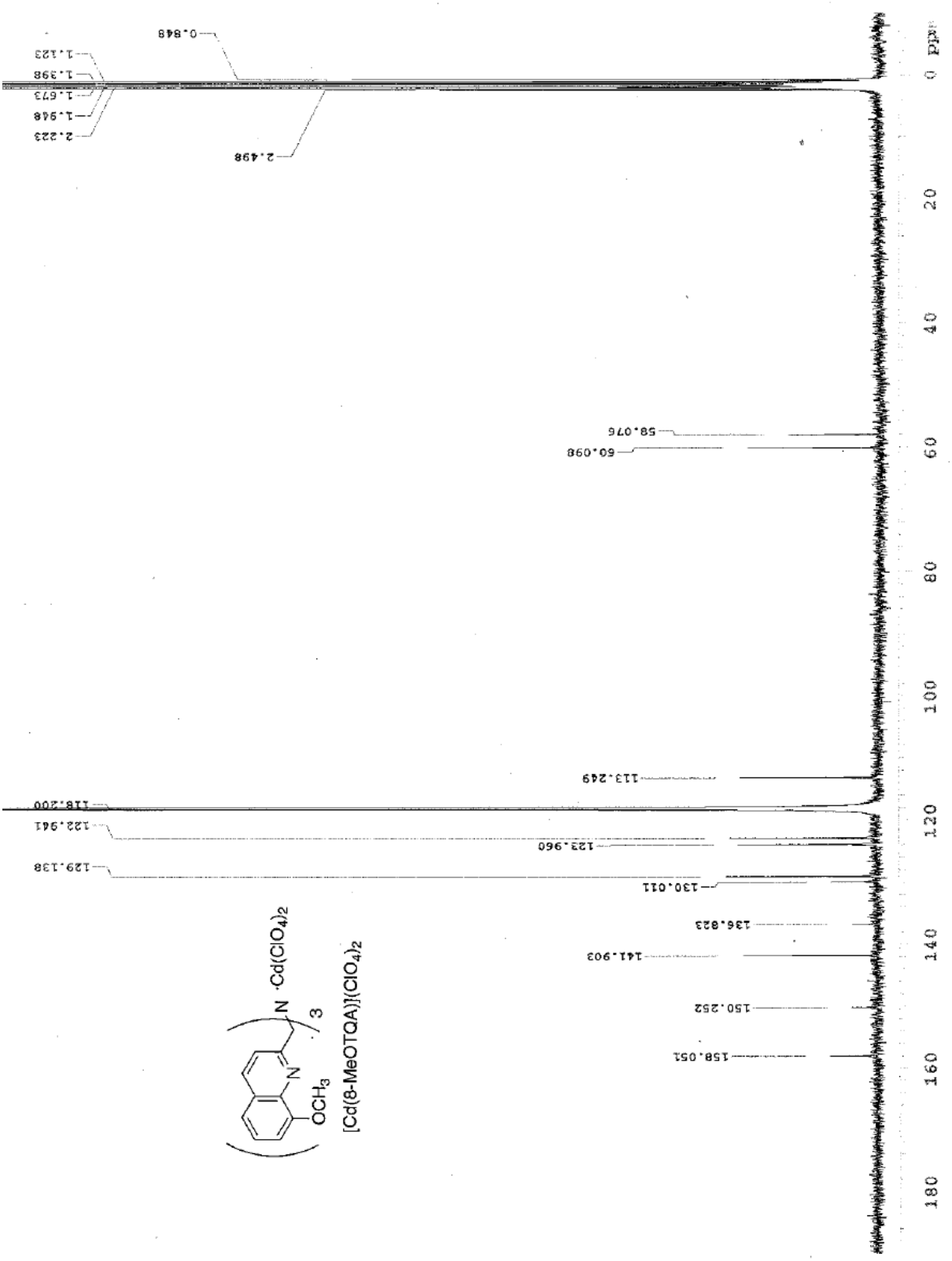

Fig. S42 ^{13}C NMR spectrum of [Cd(8-MeOTQA)]$(ClO_4)_2$ in CD_3CN.

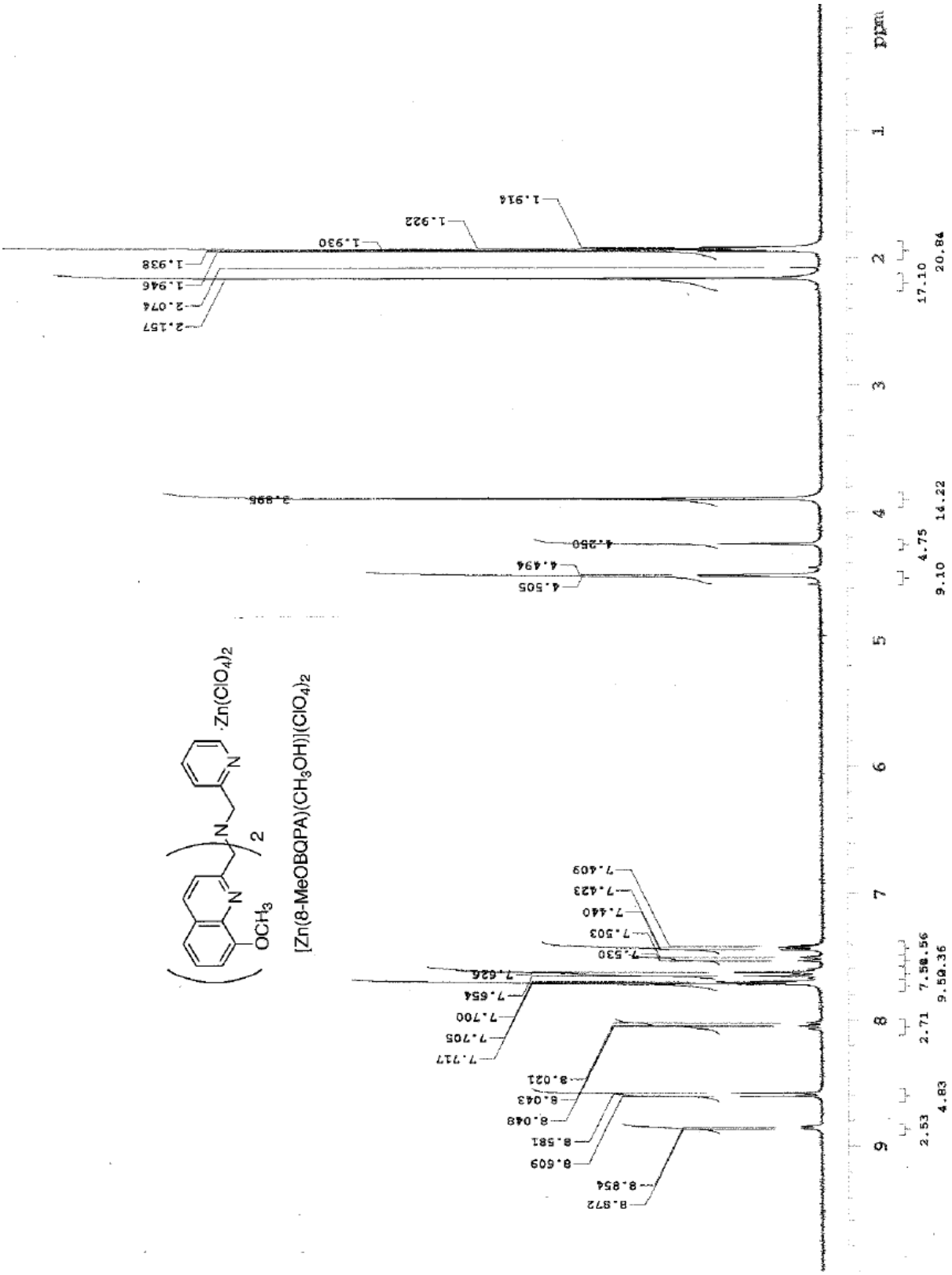

Fig. S43 ^{1}H NMR spectrum of [Zn(8-MeOBQPA)(CH$_3$OH)](ClO$_4$)$_2$ in CD$_3$CN.

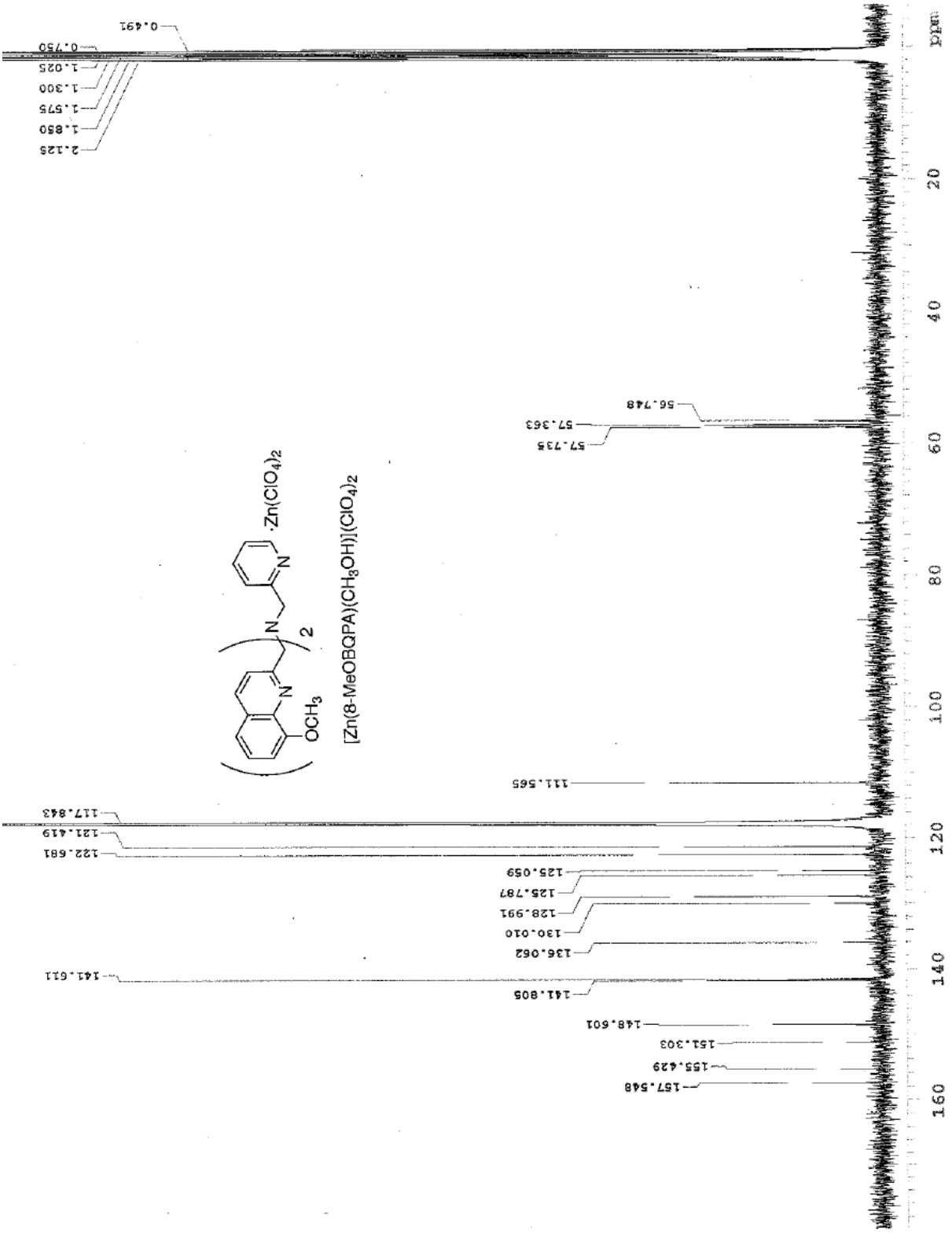

Fig. S44 ^{13}C NMR spectrum of [Zn(8-MeOBQPA)(CH$_3$OH)](ClO$_4$)$_2$ in CD$_3$CN.

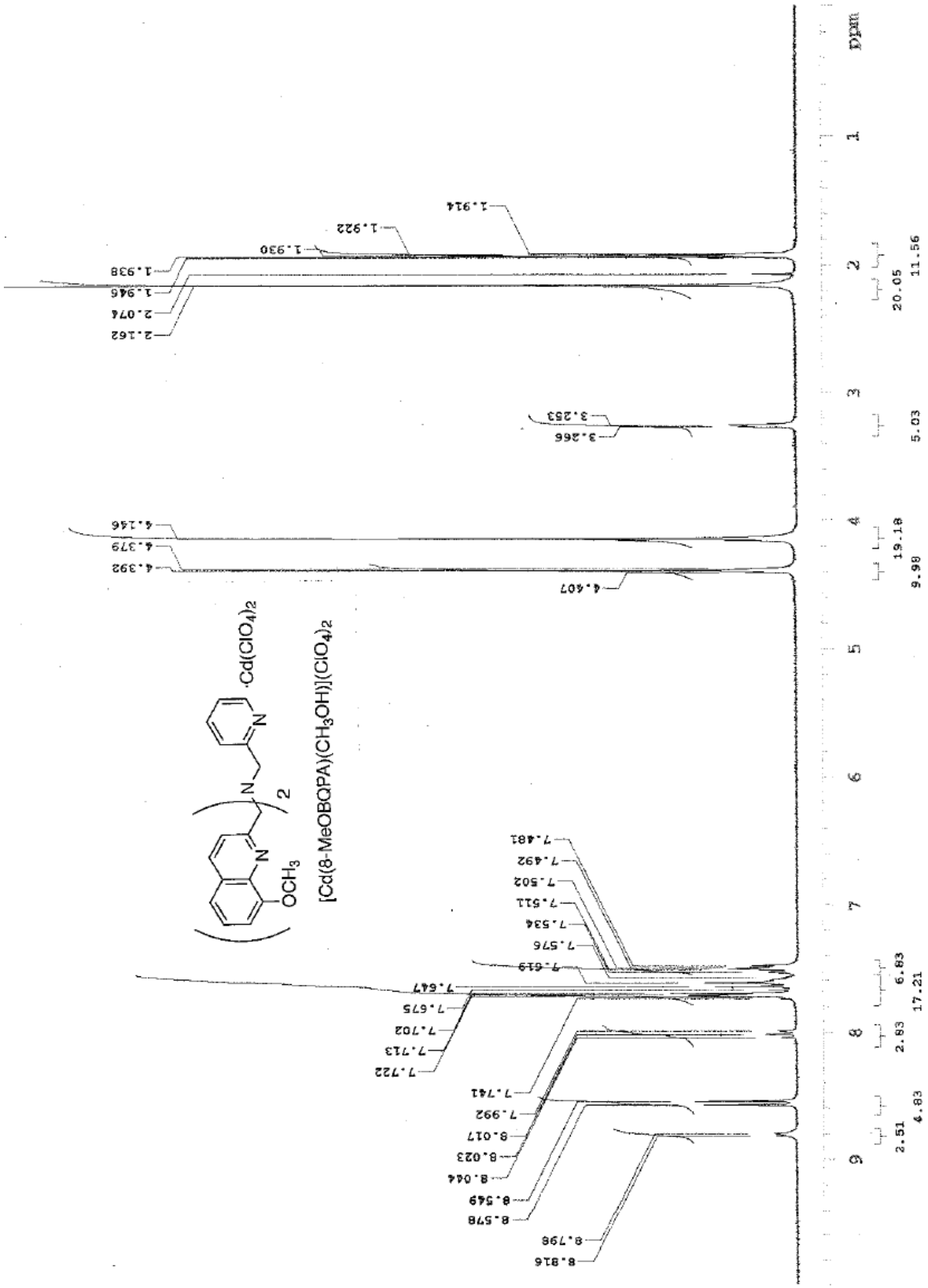

Fig. S45 ^{1}H NMR spectrum of [Cd(8-MeOBQPA)(CH_3OH)](ClO_4)$_2$ in CD_3CN.

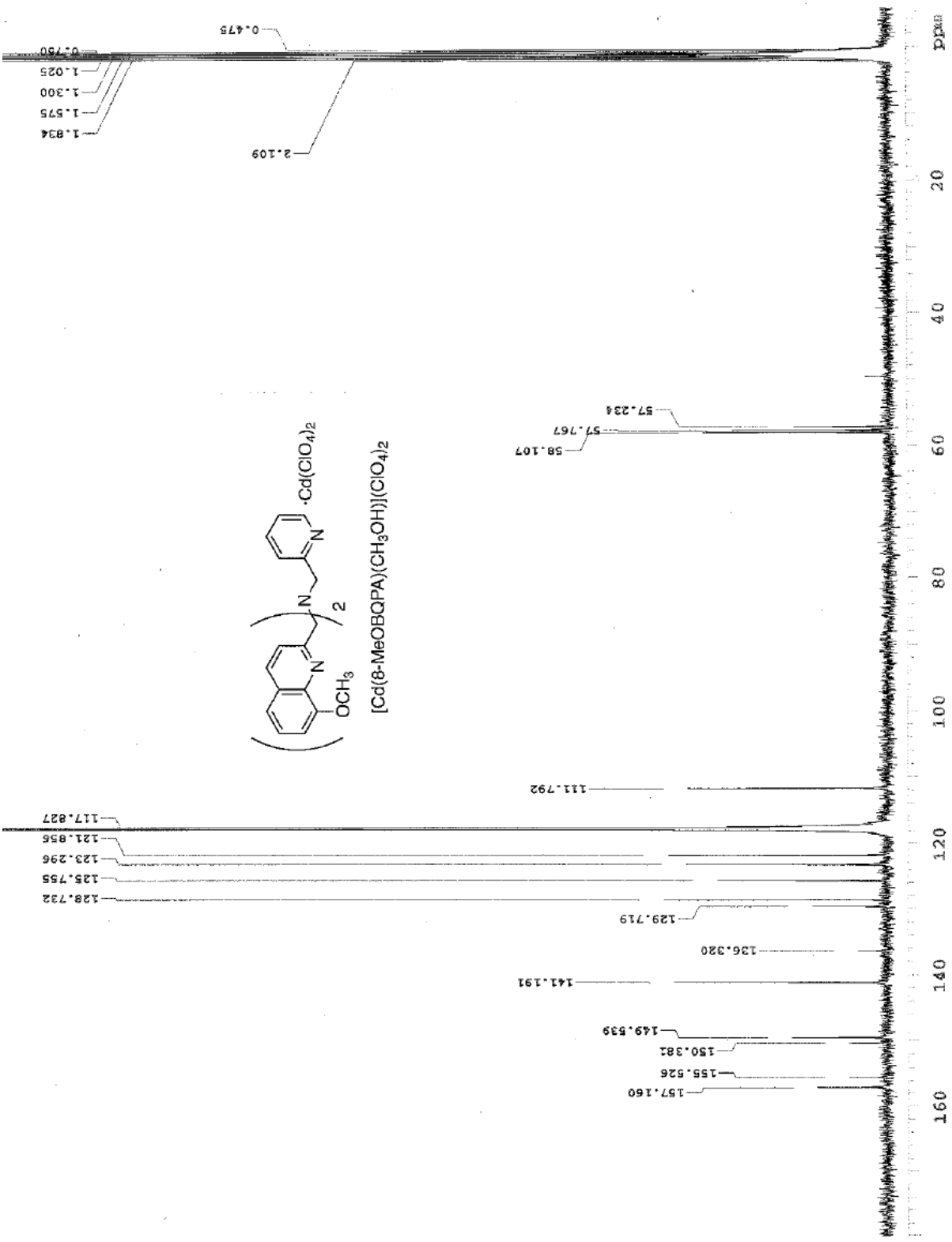

Fig. S46 ^{13}C NMR spectrum of [Cd(8-MeOBQPA)(CH_3OH)](ClO_4)$_2$ in CD_3CN.